UNIVERSITY *of the*
WESTERN CAPE

Developing a lateral flow device for the detection of novel breast cancer biomarkers

Aaron Tejada

A thesis submitted in partial fulfilment of the requirements for the degree Magister Scientiae in the Department of Biotechnology, University of the Western Cape.

Supervisor: Prof M. Meyer

Abstract

Breast cancer is the most prevalent malignancy and one of the leading causes of death in women worldwide. Delayed diagnosis of breast cancer greatly reduces the effectiveness of treatment and is considered one of the major contributing factors to its high mortality rate. Cancer treatment is most effective during the early stages of the disease, therefore the earlier that cancer is detected, the greater the chance for survival. Currently, breast cancer screening relies largely on imaging techniques such as mammography and magnetic resonance imaging (MRI) which lack sensitivity and specificity; and are both invasive, cost-intensive and are often not easily accessible to patients in low-income countries. Molecular methods such as fluorescence *in situ* hybridisation (FISH) and immunohistochemistry (IHC) have provided oncologists with more sensitive means of screening, however, these techniques proved to be costly, time-intensive, invasive and lack suitable biomarkers for their routine use as screening tools. Recent advances in the fields of bioinformatics, molecular biology and nanotechnology may provide solutions to these issues by enabling researchers to perform high-throughput screening and validation processes to identify novel and disease-specific biomarkers for rapid detection of diseases at the point of care.

A serum biomarker associated with breast cancer; UL16 Binding Protein-2 (ULBP-2) was previously identified in a Bioinformatics study. Literature suggests that ULBP-2 is cleaved from the cell surface and secreted in serum, making it an ideal candidate biomarker for less-invasive diagnostic/screening of diseases using a lateral flow assay (LFA). LFAs are relatively cheap to produce and are easy to use with minimal skill required for interpretation. They are non-invasive, sensitive and can produce results in a short turnaround time. Therefore, the aim of the study was to develop a cost-effective and rapid gold nanoparticle (GNP)-based LFA for the detection of ULBP-2.

ULBP-2 expression was evaluated by Enzyme-linked Immunosorbent Assay (ELISA) in protein samples obtained from cell lysate and culture supernatant of MCF-12A, MCF 7, HepG-2, HT-29 and HeLa cells. Only the culture supernatant of the cervical cancer cell line, HeLa contained the ULBP-2 protein. A GNP-based dipstick assay which is based on the principle of an LFA was developed and used successfully to detect recombinant ULBP-2 protein. The dipstick assay demonstrates the feasibility of developing a GNP-based LFA for the detection of ULBP-2 in a serum sample. This assay can possibly be used in the future to perform cost effective screening for cancer.

Table of contents

Keywords

Biomarkers

Breast cancer

Cervical cancer

Diagnostic

Gold nanoparticles

Lateral flow assay

ULBP-2

Declaration

I declare that *"Developing a lateral flow device for the detection of novel breast cancer biomarkers"* is my own work, that it has not been submitted before for any degree or examination in any other university, and that all the sources I have used or quoted have been acknowledged as complete references.

Signed: …….……. Date: ..23-03-2023.

Aaron Tejada

List of figures

Abbreviations

Ab - Antibody

CA – Cancer antigen

CEA – Carcinoembryonic antigen

DCIS – Ductal carcinoma *in situ*

DLS – Diffractive light scattering

EGF – Epidermal growth factor receptor

ELISA – Enzyme-linked immunosorbent assay

EMT – Epithelial to mesenchymal cell transition

ER – Estrogen receptor

FFPE – Formalin-fixed paraffin-embedded

FGF – Fibroblast growth factor

FISH – Fluorescence *in situ* hybridisation

GNP – Gold nanoparticle

HER2 – Human epidermal growth factor receptor 2

IDC – Invasive ductal carcinoma

IHC – Immunohistochemistry

ILC – Invasive lobular carcinoma

LCIS – lobular carcinoma *in situ*

LFA – Lateral flow assay

MHC – Major histocompatibility complex

MIC A/B – MHC class I chain-related proteins A and B

MRI – Magnetic resonance imaging

NKG2D – Natural killer group 2 member D

NMR – Nuclear magnetic resonance

p53 – Tumour protein 53

pRb – Retinoblastoma protein

ULBP-2 – UL16 Binding protein

VEGF – Vascular endothelial growth factor

Acknowledgements

I would like to thank my parents for their sacrifices that allowed me to get me this far and for teaching me the value of education.

A special thank you to my wife and family for their unwavering support.

I would like to thank my supervisor, Prof. Mervin Meyer for granting me the opportunity to embark on this project. Your continued support and guidance throughout the many difficulties faced during this project is appreciated.

I would also like to extend a special thank you to Dr. Nicole Sibuyi and Mr. Darius Riziki Martin. Your support and assistance have been invaluable.

A special thank you to Prof. Knoessen and the staff managing the Nanoscience programme, for your support I am grateful.

I would also like to thank The Department of Science and Innovation (DSI) and the UWC NIC Biolabels Research Node laboratory for funding this project.

Chapter 1. Literature review

1.1 Introduction

Humans have been burdened by cancer throughout recorded history; with the earliest evidence of cancer dating back to 3000 BC as demonstrated in fossilized human bone which shows evidence of cancer (Sudhakar, 2009). Cancer is currently one of the leading causes of morbidity and mortality worldwide with an estimated 19.3 million new cases and close to 10 million deaths recorded in 2020. The incidence of cancer is continuously rising with the number of cases expected to reach over 30 million per annum by 2040 (Sung *et al*., 2021).

Cancer is a group of diseases characterised by the uncontrolled proliferation of genetically modified cells. The precise cause of cancer is often indiscernible due to the complex heterogeneity of the disease. However, there are a myriad of risk factors that have been linked to cancer including genetic predisposition, viral infection, smoking and exposure to radiation (Feng & Spezia *et al.,* 2018). Although more than 200 different types of human cancers have been identified based on the organ of origin in the body; the fundamental pathophysiology of cancer remains the same in all cancer types.

The development of cancer is a complex and heterogeneous process in which a multitude of biological pathways are affected. The deregulation of three main classes of genes, namely tumour suppressor genes, DNA repair genes, and proto-oncogenes collectively contribute to the cancer phenotype (Imran & Qamar *et al.,* 2017). The onset of cancer can be triggered by genetic alterations (nucleotide deletions, insertions, or substitutions). Cells acquire several new traits through these genetic alterations. These include the ability to maintain continuous proliferative signalling, replicative potential, and angiogenesis. Cancer cells must also be able to resist tumour-suppressor genes, evade apoptosis, be able to metastasize and invade healthy tissue (Hanahan and Weinberg, 2011).

1.2 Molecular characteristics of cancer

1.2.1 Sustained mitogenic growth signalling

Molecules that stimulate cell growth (e.g., steroid hormones and vitamins) convey signals to cells that allow cells to progress through the cell cycle and this ensures normal growth and division of cells (Foroughi *et al.,* 2019). In healthy tissues, cell proliferation is controlled by a balance between the production and degradation of these growth factors via intra-cellular signalling pathways. These pathways involve among many other factors, cell-surface receptors, and a complex network of enzymes such as proteases and sulfatases (Hanahan and Weinberg, 2011). Cancer cells, however, have acquired the ability to override these regulatory signals and are thus able to proliferate continuously. Cancer cells may over-express cell-surface receptors or proteins which render the cell hyper-sensitive to growth factor signals, allowing cancer cells to proliferate continuously, even at low levels of growth factors (Hanahan and Weinberg, 2011). For example, growth factors such as the estrogen receptor (ER) and Human Epidermal Growth Factor Receptor 2 (HER2) are two of the most overexpressed growth factors in breast cancer, and are recognized as biomarkers for cancer, as well as targets for the effective treatment of cancer (Perrier *et al.,* 2018). Other strategies to sustain proliferation include the structural alteration of the cell-surface receptors, which results in ligand-independent growth signalling. In order to ensure a constant supply of growth signals, cancer cells are also able to induce autocrine signalling by producing their own growth factors. Alternatively, cancer cells can stimulate healthy cells in the tumour micro-environment to produce growth factors that will allow the cancer cells to continue to grow and multiply (Hanahan and Weinberg, 2011).

1.2.2 Unlimited replication

Healthy cells are programmed to pass through a limited number of replication cycles until they reach a non-proliferative state known as senescence. This limit is determined by the length of telomeres; regions of tandemly repeated DNA sequences at the terminal ends of chromosomes that protect the chromosomes from degradation (Shay, 2018). The progressive shortening of telomeres, due to the inability of the DNA polymerase to replicate the terminal ends of double-stranded DNA, inhibits the protective ability of telomeres allowing neighbouring chromosomes to fuse to each other which eventually results in cell death (Shay, 2018). In contrast, cancer cells can replicate limitlessly by overexpressing telomerases, which are enzymes that add telomeres at the terminal ends of chromosomes. In doing so, cancer cells maintain sufficient telomere length for unlimited replication cycles. Along with its ability to invade healthy tissue; this trait contributes significantly to the destructiveness of cancer by allowing cancer cells to develop into macroscopic tumours (Maciejowski and de Lange, 2017).

1.2.3 Chronic angiogenesis

Like healthy tissue, tumours require an efficient vascular system for the uptake of oxygen and nutrients as well as for the excretion of carbon dioxide and metabolic waste. The normal vascular system is formed during prenatal development, a process called angiogenesis, which involves the formation of new blood vessels from the existing blood vessels. In adults, angiogenesis becomes largely dormant until intermittent activation by physiological processes such as wound healing. However, due to the continuous growth of tumour tissue in cancer, angiogenesis is always activated (Aguilar-Cazares *et al.,* 2019).

There are several known strategies that cancer can deploy to carry out this chronic angiogenesis. These include the overexpression of the pro-angiogenic signal proteins, such as vascular endothelial growth factor (VEGF) and fibroblast growth factors (FGF) (Rajabi and Mousa, 2017).

The abnormal tumour vasculature is characterized by excessive blood vessel growth and capillaries that are enlarged and distorted. Increased levels of hypoxia and apoptosis in the surrounding tumour microenvironment also contribute to the leaky vasculature that is associated with tumour growth (Aguilar-Cazares *et al.,* 2019).

1.2.4 Evasion of tumour-suppressors

In addition to traits that stimulate tumour progression, cancer cells also acquire the ability to evade mechanisms of negative regulation. Examples of this are the cell cycle checkpoint controls which depend largely on the products of tumour-suppressor genes such as retinoblastoma protein (pRb) and tumour protein 53 (p53) (Martinez-Bosch *et al.,* 2018). There are several checkpoints in the cell cycle where verification of DNA occurs which ensures that damaged DNA does not propagate and become part of daughter cells. So, in addition to acquiring altered growth-controlling genes (i.e., activated oncogenes and inactivated tumour suppressor genes), many types of cancer cells have inactivated one or more of their checkpoint controls. With these controls inactivated, incipient cancer cells can rapidly accumulate (Martinez-Bosch *et al.,* 2018).

1.2.5 Evasion of apoptosis

Apoptosis, also known as programmed cell death, plays a vital role in cellular homeostasis. In physiological conditions, apoptosis prevents the progression of disease by removing damaged or unnecessary cells. During the development of cancer however, cells accumulate a series of genetic alterations that render cancer cells immune to apoptosis granting them an unlimited and unchecked proliferative potential (Sharma *et al.,* 2019). The role of apoptosis in cancer suppression or development has been well documented through functional studies and has shown to be an important trait in most cancers (Hanahan and Weinberg, 2011).

Common apoptosis evasion pathways include imbalances between pro-apoptotic and anti-apoptotic proteins, reduced caspase function, and impaired death receptor signalling (Wang *et al.,* 2017). The most commonly disrupted pathways in cancers are those dependent on p53, a tumour suppressor gene that initiates apoptosis by upregulating the expression of pro-apoptotic proteins in response to DNA breaks and other chromosomal abnormalities (Hanahan and Weinberg, 2011). Over 50% of human cancers express a defective form of the p53 gene and are thus able to evade apoptosis (Sharma *et al.,* 2019).

1.2.6 Tissue invasion and metastasis

One of the most detrimental traits of cancer is the ability of cancer cells to migrate from their site of origin to distant organs; this migration is known as metastasis. Tumour metastasis results in the expansion of cancer into regions with more nutrients and space to achieve exponential proliferation. The first step in escaping the primary tumour site is for cancerous cells to break away from the tissue where it originated by dissolving the extracellular matrix that maintains the integrity of the surrounding tissue (Chen *et al.,* 2019). This is achieved by the suppression of proteins that promote cell-to-cell adhesions such as immunoglobulins and cadherins. E-cadherin, a protein that inhibits growth after cell-to-cell adhesion, has been shown to be inactivated in migrating tumour cells or undergoes transition to a more motile and invasive phenotype (Corso *et al.,* 2020).

Tumour cells also exploit macrophages' ability to remodel matrices to invade tissues and initiate angiogenesis at the new site. Certain tumour cells have also been shown to use the epithelial to mesenchymal cell transition (EMT) pathway to initiate metastasis by transforming bound cancer cells into freely migrating mesenchymal cells. Cancerous cells that undertake this transformation are often cancer stem cells that undergo the reverse transformation once at their destination and migrate to neighbouring or distant organs (Georgakopoulos-Soares *et al.,* 2020).

1.3 Classification of breast cancer

Breast cancer is a cancer that develops in the epithelial cells of breast tissues such as lobules and ducts, and sometimes fatty and fibrous connective tissues as well. As the disease progresses, cancer cells break off from the initial tumor site and metastasize via the blood or lymphatic systems to distant organs such as the liver and lungs. Breast cancer is the most diagnosed cancer and the leading cause of cancer death among females worldwide, accounting for 58.5% of all cancer cases and 17.7% of cancer deaths in 2020 (Sung *et al.*, 2020). While among South African women, breast cancer has the highest incidence rate, and ranked the second leading cause of death after cervical cancer (Sung *et al.*, 2020). In South Africa, over 15 000 new cases of breast cancer have been diagnosed in 2020 (Ferlay *et al.*, 2021). Breast cancer places a large burden on health care systems and is equally burdening on patients, especially in low-income regions.

Breast cancer is classified based on its location within the breast tissue. The most common type is known as ductal carcinoma and originates from the epithelial cells that line the milk ducts in the breast. Tumours that originate from cells that line the lobules are known as lobular carcinoma. Less common is the breast cancer that originates from stromal tissues such as fatty and connective tissues (Zhang *et al.,* 2017).

Other rare types of breast cancer include inflammatory breast cancer which is characterized by inflammation of the affected breast; medullary carcinoma, an invasive cancer that forms a distinct boundary between tumour tissue and healthy tissue; and mucinous carcinoma which is formed by the mucus-producing cancer cells (Tsang and Tse, 2020).

Breast tumours can be further classified based on their aggressiveness and overall prognosis. Tumours that grow in localised areas and have not yet invaded nearby tissues are classified as benign or *in situ*, which generally have a better prognosis than malignant or invasive cancer tumours that invade and/or metastasize their surrounding tissues (Weinberg, 2007).

Breast cancer is generally classified into four main types: ductal carcinoma *in situ* (DCIS), lobular carcinoma *in situ* (LCIS), invasive ductal carcinoma (IDC) and invasive lobular carcinoma (ILC). Initially, a tumour may not be harmful in its benign state, but as it progresses it may become malignant and metastasize to other parts of the body via the lymphatic or circulatory systems. It is when the tumour transforms into this malignant state that it can become harmful, by invading healthy tissues and obstructing organs and blood vessels (Weinberg, 2007).

It is thus vital to detect breast cancer before the tumour reaches a malignant state, preferably during Stage 0 of breast cancer, which is defined as a pre-cancerous condition in which abnormal cells of DCIS or LCIS have not yet invaded the nearby tissues (Tsand and Tse, 2020). When detected at stage 0, the correct treatment of breast cancer can result in a 90% chance of cure (Abeloff *et al*., 2008). Survival rates of breast cancer have improved since the 1900's as a result of early cancer detection, better staging and improved treatment. However, the lack of affordable and accessible screening methods for breast cancer still presents a major burden in developing countries (Vanderpuye *et al.,* 2017).

1.4 Diagnosis of breast cancer

Breast cancer presents several features that can be used to screen and diagnose patients with or at risk of developing breast cancer. Symptoms may include but are not limited to a lump in the breast or armpit, swelling or redness of the breast, inversion or discharge from the nipple, or dimpling or flakiness of the breast skin (CDC, 2021).

Screening of breast cancer can begin with self-examination, which involves the patient looking at and feeling the breast for any abnormalities (Madhukumar *et al.,* 2017). Any symptoms that may be present can be confirmed clinically by using conventional tests, which are divided into two categories, imaging and molecular techniques as discussed below.

1.4.1 Imaging techniques

Imaging techniques have played a vital role in reducing mortality by detecting breast tumours before they become invasive. These methods are not only used to classify conspicuous breast masses, but also to determine the extent of tumour progression (Jafari *et al.,* 2018). Imaging techniques have thus been heavily relied upon for the screening and diagnosis of cancer. One of the first studies that contributed to the development of the breast imaging technique now known as mammography began in 1913, when German surgeon, Albert Salomon performed a radiological study on breast tissue specimens and demonstrated the correlation between X-ray photographs and the presence of breast cancer (Salomon, 1913).

1.4.1.1 Mammography

Mammography is an X-ray based procedure that is widely used as a screening and diagnostic test for breast cancer. It uses low-energy X-rays to visualise the patient's breast to detect tumour masses and/or micro-calcifications that are characteristic of breast cancer from a mammogram (Nyante *et al.,* 2017). Mammography is one of the best methods to date to detect breast cancer in its earliest and most treatable stage. It can detect tumours at an average of 1.7 years before the lump can be physically felt. Detection of breast cancer at a local site or where the tumour originated has been reported to have a 5-year survival rate of greater than 90%. This rate decreases to less than 50% when the disease has spread to the lymph nodes and less than 20% when it has spread to distant organs (Dange *et al.,* 2017).

There are however certain limitations to this method. Fat is radiographically translucent; therefore, X-rays are allowed to pass through it relatively unobstructed making fat appear darker on a mammogram. In contrast, epithelium and connective tissues are denser and are thus able to block X-rays more effectively, making these tissues appear lighter (Nyante *et al.,* 2017). Tumour masses and calcifications generally appear as white areas on mammograms because they absorb more X-rays; this results in the lack of contrast between the tumour mass and dense breast tissue in the background which makes it difficult to detect characteristic breast cancer masses in women who have radiographically dense breasts (Gilbert and Pinker-Domenig, 2019). Also, mammography is unable to distinguish between tumours which are benign from those that are malignant (Gilbert and Pinker-Domenig, 2019). This may result in over-diagnosis in which case a benign tumour would be treated more aggressively than required. This was confirmed by seven trials involving 6000 women, where 30% of patients with benign tumours were over-diagnosed and subsequently over-treated (Gøtzsche and Nielsen, 2009). Due to these limitations, attention has since shifted from X-ray based technologies to more complex imaging techniques such as magnetic resonance imaging (MRI) and ultrasound that can complement mammography.

1.4.1.2 Magnetic resonance imaging (MRI)

MRI is an imaging technique that uses the properties of nuclear magnetic resonance (NMR) to visualize internal structures of the body (Mann *et al.,* 2019). NMR is a phenomenon in which nuclei that are placed in a magnetic field absorb and emit electromagnetic radiation at a resonance frequency that is proportional to the magnetic properties of the isotope and the strength of the magnetic field (Mann *et al.,* 2019).

An MRI scan can generate more detailed images of the human breast than a mammogram and has the capacity to show the extent of LCIS which is often not seen in mammograms (Monticciolo *et al.,* 2018). MRI can detect breast cancer early with up to 90% sensitivity (Monticciolo *et al.,* 2018). Although the MRI scan is highly sensitive, it has low specificity. Another drawback of MRI is the high cost. While a mammogram costs just under R2 000, an MRI scan can cost between R3 000 and R15 000 at some medical centres (Parklane Radiology, 2021). MRI is thus not recommended to replace mammography but should be used as a complementary screening test (Bickelhaupt *et al.,* 2017).

1.4.1.3 Ultrasonography

Ultrasonography is an imaging technique that uses sound waves that are above the receptive range of human hearing (between 2 and 20 MHz) to visualise the internal structures of the body (Christensen-Jeffries *et al.,* 2020). Like MRI, this technique is intended to serve as a supplement to mammography for the evaluation of breast abnormalities (Geisel *et al.,* 2018). Ultrasonography can differentiate between cystic and solid masses. It also aids in differentiating between benign and malignant tumours and thereby helps overcome some of the challenges faced by mammography (Geisel *et al.,* 2018).

Ultrasonography has shown up to 97% sensitivity in breast cancer detection when used adjunctively with mammography. An improvement in sensitivity for dense breasts was also observed using ultrasonography compared to mammography (Rebolj *et al.,* 2018). However, ultrasonography faces a few drawbacks of its own, including the inability to demonstrate micro-calcifications. The accuracy of this technique is also highly operator-dependent and requires skilled radiologists for interpretation of the results (Zanotel *et al.,* 2018).

In order to minimize the error rate of individual diagnostic methods, oncology clinicians have suggested a combination of mammography, MRI, and ultrasonography (Bickelhaupt *et al.,* 2017). Since MRI and ultrasonography are not based on X-rays, these techniques will not succumb to the same drawbacks as mammography. However, the combination of diagnostic methods leads to a significant increase in cost due to specialised equipment and the requirement for skilled radiologists to analyse and interpret the results. Most importantly this would increase the cost for patients; approximately R1 500 for mammography, R 500 for ultrasonography, and R 5 000 for MRI which is not practical in a middle to low-income country like South Africa, with significant disparity in income between rural and urban areas (OECD, 2013). There is thus a need for cost-effective diagnostic screening tools that can be reliably used to screen for breast cancer at the early stages of the disease before more expensive diagnostic tests are used to confirm the diagnosis.

1.4.2 Molecular techniques used to detect breast cancer

1.4.2.1 Immunohistochemistry (IHC)

IHC is a technique that relies on the binding specificity between an antibody and an antigen and is used to detect and localize specific antigens within a tissue sample (Magaki *et al.,* 2019). The antibody is usually tagged with a contrast agent that will generate a coloured or fluorescent signal; examples include horseradish peroxidase which catalyses a colour-producing reaction after the addition of a chromogenic substrate. If antigen-antibody binding occurred within a tissue specimen, the location and relative amount of the target antigen can be visualized by light microscopy (Magaki *et al.,* 2019). IHC is most commonly used to measure the extent of Human epidermal growth factor receptor 2 (HER-2) expression in formalin-fixed paraffin-embedded (FFPE) breast cancer tissue samples by introducing antibodies against the HER-2 receptor (Ann *et al.,* 2020).

Studies have shown a good correlation between gene copy number and HER-2 receptor levels when the IHC test is performed on FFPE tissue samples (Ann *et al.,* 2020). IHC testing is widely used due to its relatively low cost, availability, simplicity of the equipment required for analysis, and the ability to preserve slides for future reference. However, there are limitations with IHC, which included the cross-linking of antigen sites due to prolonged fixation, degradation of antigens due to prolonged storage, lack of a positive internal control signal, and inter-observer variation in the interpretation of results which may be due to the type of antibody used (polyclonal or monoclonal) and the type of scoring system used in analysis (Tan *et al.,* 2020).

HercepTest is the most widely used scoring system which uses a US FDA-approved polyclonal antibody whose antigenic domain recognizes the internal domain of the HER-2 receptor (Jørgensen and Winther, 2019). According to this scoring system, a negative result is reported with 0 and 1+ staining (no staining and partial staining of membranes in at least 10% of cells, respectively), while 2+ and 3+ staining is reported as HER-2 positive test (moderate and complete staining of membranes in at least 10% of cells, respectively) (Jørgensen and Winther, 2019). This scoring system has been criticised because patients whose results were reported as 2+, HER-2 gene amplification was shown in only 25% of the cases (Shneider *et al.,* 2019). Thus, it has been suggested that tests scored as 2+ should not be considered as positive but instead, a borderline value, and that it must further be confirmed by FISH whether a patient is HER-2 positive (Shneider *et al.,* 2019).

1.4.2.2 Fluorescence *in situ* Hybridisation (FISH)

FISH is a technique whereby fluorescent DNA probes are used to detect and localize the presence of specific DNA or RNA target sequences in cells or tissue specimens.

The hybridisation of the probe to its complementary DNA sequence can be detected by fluorescence microscopy (Ratan *et al.,* 2017). While a healthy cell contains 2 copies of the HER-2 gene and 4 copies during mitosis; a cancerous cell contains more than 4 copies of the HER-2 gene. The FISH test can thus be used to quantify the level of HER-2 gene in a cell and thereby determine the HER2-status of a tumour (Ahn *et al.,* 2020).

Pathvysion is the most commonly used FISH test procedure and makes use of FFPE breast cancer tissue specimens obtained by biopsy (Bogdanovska-Todorovska *et al.,* 2018). Following fixation, the cells are permeabilised to allow probes to gain access to target nucleic acids. A fluorescently labelled probe which is gene (HER-2)-specific is allowed to hybridize to its target. Subsequent hybridisation steps can then be visualised by fluorescence microscopy (Bogdanovska-Todorovska *et al.,* 2018). FISH was shown to be superior to IHC in the detection of breast cancer, particularly in cases where moderate (2+) staining was observed. DNA probes used in FISH are less susceptible to the problems of fixation and storage than the antibodies used in IHC due to the relative stability of DNA (Agersborg *et al.,* 2018). However, FISH uses organic fluorophores as probes which have drawbacks of their own. Although FISH can visualize multiple cancer biomarkers simultaneously through different fluorescence tags, the spectral overlap of conventional fluorophores limits the number of probes that can be distinguishable based on colour. Multiplexing usually complicates the interpretation of results as the number of fluorophores increases (Agersborg *et al.,* 2018). Furthermore, the multiple wavelengths required to excite the variety of fluorophores emitting at different wavelengths introduces chromatic abnormalities that may impair the integrity of these probes. There is also difficulty in deciphering background fluorescent signals (Huber *et al.,* 2018). FISH also presents an increase in cost relative to IHC testing due to the specialised equipment required for detection of fluorescence and is thus only used as a last resort.

1.4.2.3 Enzyme linked immunosorbent assay (ELISA)

The ELISA is a powerful tool used for detecting and quantifying specific analytes in a complex mixture. Originally described by Engvall and Perlmann (1971), the method was developed as a replacement for radioimmunoassay. A typical ELISA is shown in Figure 1.1 (Leinco Technologies, 2022). It is a plate reader-based assay where an antigen-capture antibody is immobilised on a surface, and when an antigen binds to it, it can be detected by a colorimetric signal generated by binding of a labelled detection antibody to the antigen-capture antibody-antigen complex. The relative simplicity and robustness of ELISA has revolutionized the field of immunology and has resulted in its widespread application in the fields of microbiology and oncology among others (Tan *et al.,* 2017). ELISA also has commercial applications in the detection of disease markers and allergens in the diagnostic and food industries, respectively.

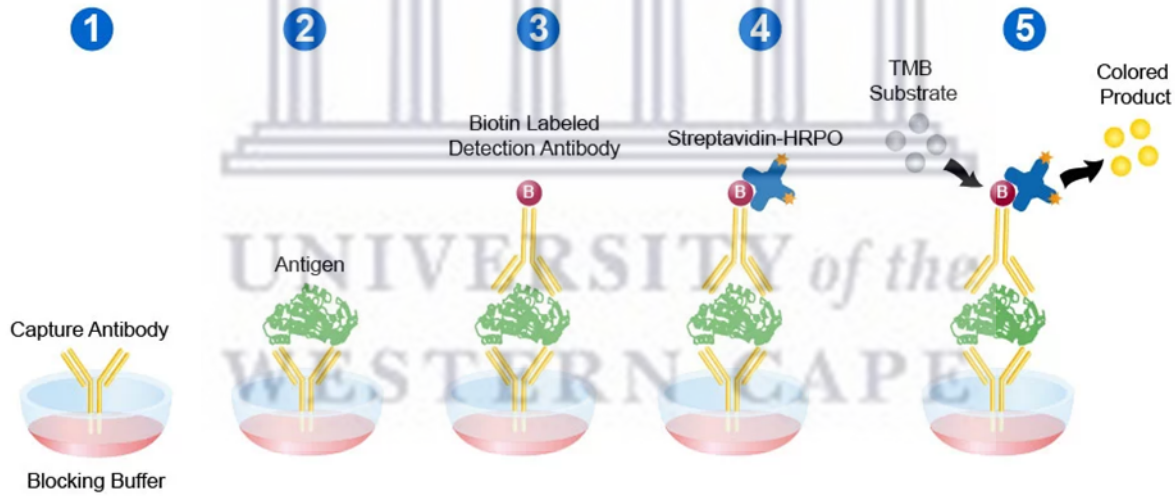

Figure 1.1: Schematic representation of a sandwich ELISA. The assay consists of two antibodies, a capture antibody which binds to and captures the antigen and a biotin labelled detection antibody which binds to a different site on the antigen. An enzyme is then bound to the labelled antibody and a substrate is added which digests the substrate and allows for colorimetric detection of antigen in a sample.

ELISA is highly specific, can detect antigens at ultra-low concentrations and is safer than radioimmunoassay for a wide variety of tests (Ono *et al.,* 2018). Many enzyme detection methods involved in ELISA use standard spectrophotometric detection, which eliminates the need for other sophisticated and expensive equipment (Liu *et al.,* 2020). However, ELISA assays that depend on antibodies have various downsides. In addition to batch-to-batch variations in the production of antibodies, it is tedious and challenging to generate specific monoclonal antibodies, especially against non-immunogenic molecules (Ono *et al.,* 2018).

1.5 Lateral flow assays

Recent advancements in Lateral Flow Assay (LFA) technology have paved the way for more cost-effective, rapid, and sensitive diagnostic assays, which are suitable for use in low-income countries with limited resources. These systems are user-friendly and can be operated in non-clinical settings at point-of-care (POC) by non-health professionals; most importantly, the results are visual and easy to interpret. LFAs are used in several industries including, medical, industrial, and food industries for the detection of infectious diseases, toxic substances, and food-borne pathogens to name a few.

To perform an LFA, one would typically apply a sample to the sample pad, the sample migrates through the conjugation pad to the test and control zones where the analyte interacts with the immobilized capture antibodies. In the presence of the analyte, two visible lines will appear in both the test and control zones, while a single line in the control zone only represents a negative test (Boehringer and O'Farrell, 2022). LFAs can be subdivided into two types based on the mechanism of detection as discussed below.

1.5.1 Direct LFA

A direct (or non-competitive) LFA is normally used for larger analytes with multiple binding sites where the analyte will be sandwiched between two complementary antibodies (Chen *et al.,* 2020). The reporter molecule (e.g., GNP or fluorescent dye) bound to a detection antibody is temporarily immobilized on the conjugate pad. The primary antibody which captures the target analyte is adsorbed on the test line of the strip while a secondary antibody that captures the reporter-antibody conjugate is adsorbed to the control line. Once the sample is applied to the sample pad it migrates laterally throughout the length of the strip via capillary action. If the sample contains the target analyte; it will be captured by the reporter-antibody conjugate which results in the formation of an antibody-target complex (Van Amerongen *et al.,* 2020). At the test line, antibody-target complex will be captured by the primary antibody and in doing so; the analyte becomes sandwiched between the two antibodies. Excess antibody-target complex will be captured at the control line by the secondary antibody. Thus, a signal at both the test and control lines would indicate a positive result, while a negative result would be indicated by a signal on the control line only (Van Amerongen *et al.,* 2020).

1.5.2 Indirect LFA

Indirect (or competitive) LFA is best suited for low molecular weight compounds which cannot bind two antibodies simultaneously (Koczula and Galotta, 2016). The absence of colour at the test line is an indication of the presence of an analyte while the appearance of colour both at the test and control lines indicates a negative result (Van Amerongen *et al.,* 2020). Indirect LFA has two layouts. In the first layout, solution containing target analyte is applied onto the sample pad, and the prefixed labelled biomolecule conjugate gets hydrated and starts flowing along the strip. Test line contains pre-immobilized antigen (same analyte to be detected) which binds specifically to labelled conjugate. The control line contains pre-immobilized secondary antibody which can bind to the labelled antibody conjugate.

When the sample reaches the test line, immobilized antigen will bind to the labelled conjugate. Antigen in the sample solution and the one which is immobilized at test line of strip compete to bind with labelled conjugate (Van Amerongen *et al.,* 2020). This indirect or competitive layout is depicted in Figure 1.2, where the analyte, β-lactam competes with β-lactam immobilized on the test line for the GNP-bound receptor antibody (Li *et al.,* 2021). In another layout, labelled analyte conjugate is dispensed at the conjugate pad while a primary antibody to analyte is dispensed at test line. After application of analyte solution, competition takes place between analyte and labelled analyte to bind with the primary antibody at the test line.

While LFAs have the potential for application for breast cancer screening at the POC, reliable biomarkers for the detection of breast cancer from sera samples do not exist. Ideally these should be molecules that can be strongly associated with the disease and are present in the serum of breast cancer patients, but not healthy individuals.

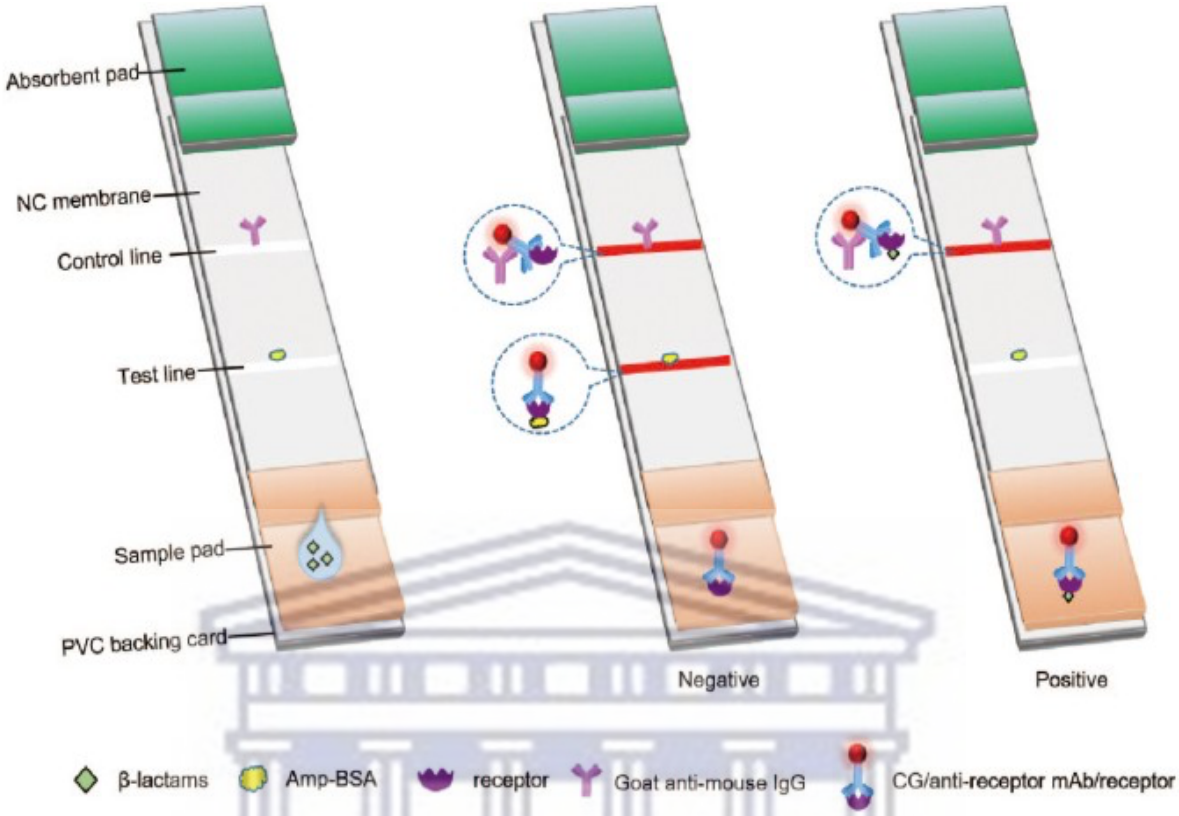

Figure 1.2: Schematic representation of the basic principle of an indirect LFA. Sample flows from the sample pad through to the absorbent pad. A negative result is indicated by a colour signal at the test line while a positive result shows no colour at the test line, this is due to the target in the sample outcompeting the immobilized target (Amp-BSA) on the test line.

1.6 Biomarkers in diagnostics

In recent years, the knowledge base surrounding the molecular mechanisms of cancer has been expanded considerably. In an attempt to circumvent many of the issues faced by the imaging techniques such as mammography which was previously mentioned and relies solely on the physical manifestations of breast cancer, researchers are leaning more towards the use of the molecular techniques to produce cheaper, more accurate, and less-invasive methods for early-stage breast cancer diagnosis (Rakha and Green, 2017).

These molecular methods rely on biomarkers (genes or gene products) which serve as indicators of a particular biological state (i.e., diseased vs healthy) and by evaluating their expression or presence in a patient sample a diagnosis can be made. Biomarkers thus serve as quantifiable traits that are helpful not just in early diagnosis, but for high-risk identification, selection of the best treatment regiment, and monitoring response to a particular treatment (Nicolini *et al.,* 2018).

1.6.1 Biomarker discovery

The identification of novel biomarkers can be achieved via several approaches which basically aim to look for molecular fingerprints that are associated with a particular disease state. Transcriptomics and proteomics are two of the most common technologies used to identify such molecular fingerprints. Transcriptomics is used to identify and quantify the levels of mRNA transcripts which encode for genes, while proteomics is used to identify and quantify proteins that may be up or down regulated during the disease. These technologies are often used in together with Bioinformatics to analyse large data sets to identify molecular signatures that can serve as biomarkers for disease states. Bioinformatics involves the use of computational approaches to collect, store and analyse large biological data sets.

Bioinformatics has provided a wealth of useful information on the characteristics of several types of cancers which can be used towards better diagnostic methods (Rakha and Green, 2017). Cancer is the result of the accumulation of multiple mutations. Due to the highly complex nature of cancer, this disease cannot be diagnosed using a single biomarker, but instead a panel of biomarkers should be used (Liu *et al.,* 2017). Platforms for biomarker discovery must therefore be able to screen a large array of potential biomarkers and diagnostic tests should be able to detect a panel of biomarkers.

Proteomics analysis of the tear fluid and nipple aspirate of breast cancer patients was used to identify two panels of biomarkers, which in turn could be used to differentiate between healthy controls and breast cancer patients with a specificity and sensitivity of at least 70% (Lebrecht *et al.,* 2009, Mannello *et al.,* 2009). A protein microarray is another high-throughput method (analogous to DNA microarray) used to track the interactions and activities of proteins as well as determine their functions (Zhu and Qian, 2012). Protein microarrays are highly sensitive, rapid, automated and economical, only requiring small quantities of samples and reagents for analysis. These tools (proteomics and genomics) have played a significant role as a data bank for *in silico* studies. Recent studies using computational tools (bioinformatics) have led to identification of several biomarkers in a fraction of the time without the need for complex experiments (Deng *et al.,* 2019).

1.6.2 Classes of biomarkers

Virtually any biomolecule (DNA, RNA, protein, lipid or carbohydrate) or metabolite which is altered during cancer development has the potential to be a cancer biomarker. As cancer cells develop, grow and multiply, changes occur which can affect the genetic structure and the product (proteins) of the affected genes. This can also affect other biomolecules and metabolites. These biomolecules and metabolites can be detected in the tissue, blood, urine, or stool of individuals who have the disease. However, many of these biomolecules and metabolites do not fit the ideal biomarker profile, due to their lack of sensitivity and specificity (Seidel *et al.,* 2017).

Biomarkers have value in different applications and can serve as either diagnostic or prognostic markers. While diagnosis refer to the detection of the disease state, prognosis is a determination of how the disease will progress. Some biomarkers are not cancer-specific, but are associated with several types of cancer; while others, with as few as one type (Jayanthi *et al.,* 2017).

However, no one biomarker is specific for cancer type, and may also be associated with non-neoplastic diseases as well. Biomarkers can be in a form of enzymes, isoenzymes, hormones, specific cell membrane proteins, oncofoetal and cell-specific antigens, carbohydrate epitopes, oncogenes, etc. (Echle *et al.,* 2021). There are only a handful of well-established tumour markers that are being used by physicians, however there are many other potential markers that are still being researched (Seidel *et al.,* 2017).

1.6.3 Biomarkers associated with breast cancer

The characteristics of an ideal biomarker include that it will be useful in the staging and prognosis of cancer, estimation of tumour burden, monitoring of the effects of therapy, detection of the risk of recurrence, and localization of tumours (Echle *et al.,* 2021). Although molecular techniques delivered promising diagnostic tests for breast cancer, the lack of selective diagnostic biomarkers is a significant limiting factor (Seidel *et al.,* 2017). Currently validated and clinical biomarkers for breast cancer include Human Epidermal growth factor Receptor 2 (HER2), Estrogen Receptor (ER), Progesterone Receptor (PR), Cancer Antigen 15.3 (CA 15.3), Cancer Antigen 27.29 (CA 27.29), Carcinoembryonic Antigen (CEA) and mucin-1 (MUC-1) (Nicolini *et al.,* 2018).

HER-2 is an oncogene-encoded growth factor receptor (homologue of epidermal growth factor (EGF) receptor), also known as c-erbB-2. It is overexpressed in breast cancer as a result of HER-2 proto-oncogene amplification. It can be measured in a tissue biopsy either by immunological assays or qRT-PCR. The presence of HER-2/neu is generally associated with a more aggressive growth and poorer prognosis for breast and ovarian cancers (Loibl and Gianni, 2017). It can also help to determine treatment options, predicting an enhanced survival benefit from Herceptin (trastuzumab) treatment, a HER-2-targeted therapy (Horton, 2002). In both pre- and postmenopausal women, knowing the levels of steroid receptors (ER and PR) can be used to predict which women are likely to benefit from hormone treatment.

Measurements of ER and PR are recommended and used in the diagnosis, prognosis, and treatment planning for women with breast cancer. Most breast cancers in post-menopausal women are ER-positive, meaning that these tumours require estrogen to grow. These ER positive breast cancers are less aggressive than ER negative breast cancers, which are generally found in premenopausal women (Yin *et al.,* 2020).

CA 27.29 is elevated in patients with breast carcinoma, but also in patients with ovarian or lung cancer, benign breast disease, cirrhosis and hepatitis, as well as women in the 1st trimester of a pregnancy (Jeong *et al.,* 2020). CA 27.29 is a glycoprotein belonging to the mucin family and is associated with the early detection of recurrent breast carcinoma. For recurrent breast carcinoma, CA 27.29 has a sensitivity of ~57% and a specificity of ~87% (Jeong *et al.,* 2020). CA 27.29, however, lacks the required sensitivity and specificity for routine detection of breast cancer and does not discriminate patients with early carcinoma from those with benign breast disease (Jeong *et al.,* 2020).

CEA is a cell surface glycoprotein, and it is a marker for colorectal, gastrointestinal, lung, and breast carcinomas (Wang *et al.,* 2017). CEA is most useful in monitoring disease therapy (as declining levels correlate with decreasing tumour burden) and has been useful in detecting the recurrence of colorectal cancer. High CEA levels in breast cancer do not correlate with grade of tumour but are useful for monitoring therapy and detecting recurrence (Wang *et al.,* 2017). Most of these markers have a good prognostic value and aid oncologists in determining the most effective treatment regime, however, they have little use as diagnostic markers due to a lack of sensitivity and selectivity (Barzaman *et al.,* 2020). Researchers continue working on specific molecular pathways involved in oncogenesis, tumour response, tumour progression, etc. to discover new molecular markers that can potentially be routinely used in medical practices of breast cancer diagnosis and therapy.

1.7 ULBP-2 as a potential biomarker for breast cancer

A Bioinformatics study which involved microarray database mining to identify cell surface biomarker proteins that are differentially expressed in breast cancer patient samples led to the identification of UL-16 binding protein-2 (ULBP-2) as a potential breast cancer biomarker protein (Ngcoza, 2013). ULBP-2 belongs to a family of proteins that are known as natural killer group 2D (NKG2D) ligands. ULBP-2 is over expressed in transformed cancer cells to facilitate the recognition and elimination of the cancer cells by Natural Killer (NK) cells via the NKG2D-mediated tumour immunosurveillance system. However, cancer cells counteract the immunosurveillance system by releasing these NKG2D ligands. Waldhauer and Steinle (2006) were the first to show that ULBP-2 is released from cancer cells and can be detected in the sera of patients with hematopoietic malignancies. Several other studies suggested that ULPB-2 is a potential cancer biomarker. Yamaguchi *et al.,* (2012) found that soluble ULBP-2 was present in the supernatants of cultured non-small-cell lung cancer (NSCLC) cells, as well as in the serum of NSCLC patients. Kegasawa *et al.*, (2019) found that soluble ULBP-2 was detected in the supernatants of pancreatic cancer cells and that the presence of this protein in the serum of stage IV pancreatic cancer patients was associated with poor overall survival.

The NKG2D receptor is a lectin-like type 2 transmembrane glycoprotein that is expressed on the surface of most human immune cells including NK Tcells, $CD8^+$ T cells and $\gamma\delta^+$ T cells (Frazao *et al.,* 2019). The NKG2D receptors along with its ligands play a crucial role in stimulating immune responses against several cellular stresses including DNA damage, pathogen infection, and tumour transformation (Frazao *et al.,* 2019).

There are several human NKG2D ligands that form part of two families of major histocompatibility complex (MHC) class I-related cell surface molecules, namely the MHC class I chain-related proteins A and B (MICA/B) and six ULBPs (ULBP1–6) (Dhar and Wu, 2018). Upon recognition of NKG2DL, the NKG2D-positive immune effector cells can initiate an immune response against NKG2DL-expressing tumour cells. However, malignant cells have developed several strategies allowing them to evade recognition by the immune system. Strategies such as NKG2DL attenuation among other mechanisms, involve the inhibition of NKG2DL transcription through the signal transducer and activator of transcription 3 (STAT3) (Ding *et al.,* 2018). One of the best described methods of immune evasion adopted by tumours is the proteolytic shedding of NKG2DL from the cell surface. This method greatly reduces the amount of NKG2DL on the tumour cell surface thereby enabling immune evasion; while the ability of the soluble NKG2DL to be internalized by the NKG2D receptor ensures escape from the immune system (Liu *et al.,* 2019). The fact that NKG2DL is shed by cancer cells and is present in the sera of cancer patients means that it can be used as an indicator for the presence of tumour cells.

The ULBP-2 gene encodes an MHC I-related molecule that binds to the NKG2D receptor on NK cells to trigger an immune response by releasing cytokines and chemokines that contribute to the recruitment and activation of NK cells (Dermikol *et al.,* 2017). The encoded protein undergoes further processing to generate the mature protein that is either anchored to the cell membrane via a glycosylphosphatidylinositol moiety, or secreted. Malignant cells secrete the encoded protein to evade immunosurveillance by NK cells (Liu *et al.,* 2019).

Transcription of ULBP-2 is induced in response to hyperproliferation and DNA damage. Moreover, NKG2DLs including MICA/B and ULBP-2 are cleaved from the cell surface by ADAM10, ADAM17 and MMP14, members of the disintegrin and metalloproteinase (ADAM) family, the levels of which correlate with poor survival of cancer patients (Dermikol *et al.,* 2017).

In addition to proteolytic cleavage from the cell surface, NKG2DLs such as ULBP-2 have also been found to be excreted in exosomes (Zingoni *et al.,* 2020). Tumours may use combinations of mechanisms to downregulate the expression of NKG2DLs. Malignant gliomas were shown to use transforming growth factor-β and metalloproteinases to reduce the expression of NKG2Ls (Zingoni *et al.,* 2020). In summary, various signals and pathways, many of which are associated with tumorigenesis and infections, regulate the gene expression of NKG2DLs at different levels.

1.8 Aims of this study

The aims of the study were to investigate if ULBP-2 is a potential diagnostic marker for breast cancer and to develop a LFA for the detection of ULBP-2.

1.9 Objectives of this study

- The objectives of this study were to screen several mammalian cancer cell lines, including a breast cancer cell line and a non-cancerous breast cell line for ULBP-2 protein expression.
- To develop a gold nanoparticle-based LFA for detection of ULBP-2 protein in lysates and supernatants obtained from mammalian cancer cell line cultures.

Chapter 2. Materials and Methods

2.1 Materials and suppliers

Chemicals	Supplier details
2X Trypsin	Thermo Fisher Scientific, USA
Coomassie brilliant blue R-250	
Dithiothreitol (DTT)	
Fetal Bovine Serum (FBS)	
4-(2-hydroxyethyl)-1-piperazineethanesulfonic acid (HEPES)	
MagicMark™ XP western protein standard	
Pierce™ unstained protein MW marker	
Bis-acrylamide	Bio-Rad, USA
Bovine insulin	Whitehead Scientific, SA
Bovine serum albumin	Sigma-Aldrich, St Louis, USA
Benzonase	
Bromophenol blue	
Glycerol	
Glycine	
Hydrocortisone	
Monopotassium phosphate	
TEMED	
Tween 20	
Hydrochloric acid	

Dulbecco's Modified Eagle's medium (DMEM) Dulbecco's Modified Eagle's medium and Ham's F12 medium (DMEM-F12) Penicillin-Streptomycin (Pen-Strep)	Invitrogen, USA
Ethanol	Kimix, SA
Human epidermal growth factor (EGF) Human ULBP2 Antibody	R&D Systems, USA
Phosphate buffer saline (PBS)	Lonza, Germany
Potassium chloride (KCl) Sodium chloride (NaCl) Sodium deoxycholate Tris(hydroxymethyl)aminomethane (Tris) Paraformaldehyde Ammonium persulfate Sodium dodecyl sulfate (SDS) Sodium hydroxide	Merck, Germany

2.2 List of kits

Qubit® Protein Assay Kit	Invitrogen, USA
Human ULBP-2 DuoSet ELISA kit	R&D Systems, USA

2.3 Buffers and solutions

RIPA Buffer: 50 mM NaCl, 50 mM HEPES (pH 7.4), 0.5 % Sodium deoxycholate, 0.1 % SDS and 1U/ml Benzonase prepared in distilled water.

0.625 M Tris-HCl: 7.6 g Tris dissolved in 1L distilled water and the pH was adjusted to 6.8 using NaOH and HCl.

1 X PBS: 8 g Sodium chloride, 0.2 g Potassium chloride, 1.44 g Disodium phosphate and 0.24 g Monopotassium phosphate prepared in 1L distilled water, and the pH was adjusted to 7.4.

1.875 M Tris-HCl: 22.7 g Tris dissolved in 1L distilled water, and the pH was adjusted to 8.8

10 % SDS: 10 g SDS dissolved in 1L of distilled water

2X Sample buffer: 10 % SDS, 25 % Glycerol, 1 M Tris (pH 6.8), 1 % Bromophenol blue and 100 mM DTT.

4 % Paraformaldehyde: 4 g of Paraformaldehyde prepared in 100 ml distilled water and the pH was adjusted to 7.2.

TBS-Tween: 2.4 g Tris, 8.8 g NaCl and 0.1% Tween 20 prepared in 1L distilled water and the pH was adjusted to 7.4.

Staining solution: 0.4 g Coomassie blue dissolved in a mixture of methanol (200 ml) and acetic acid (200 ml).

De-staining solution: 100 ml of 40% (v/v) methanol and 100 ml of glacial acetic acid made up to 1L with distilled water.

2.4 Methods

2.4.1 Cell culture and maintenance

2.4.1.1 Cell culture

Five mammalian cell lines was previously acquired from American Type Culture Collection (ATCC; Manassas, USA) by the Department of Biotechnology (UWC). Stocks of the cell lines were obtained from storage and cultured as per the suppliers' instructions. MCF-12A (ATCC no. CRL-10782) and A549 (ATCC no. CCL-185) cells were cultured in Dulbecco's Modified Eagle's medium (DMEM) F12 medium. MCF-7 (ATCC no. HTB-22) and HepG-2 (ATCC no. HB-8065) cells were cultured in Eagle's Minimum Essential Medium (EMEM). HT-29 (ATCC no. HTB-38) and HeLa (ATCC no. CCL-2) cells were cultured in DMEM. All media were supplemented with 10% Fetal Bovine Serum (FBS) and 100 IU Penicillin-Streptomycin (Pen-Strep). DMEM-F12 media for MCF-12A cells was also supplemented with 20 ng/ml Human Epidermal Growth Factor (EGF), 0.01 mg/ml Bovine Insulin and 500 ng/ml Hydrocortisone.

2.4.1.2 Starting cell culture from frozen cells

Vials containing frozen cells were removed from the -150 °C freezer and allowed to thaw at 25 °C. The cells were transferred into sterile 15 ml tubes containing 3 ml of their respective growth media as described in section 2.4.1.1 and centrifuged at 3 000 x*g* in an Eppendorf microcentrifuge for 3 min. The supernatant was discarded, and the cell pellets were re-suspended in 5 ml of appropriate growth media. The latter was transferred into sterile 25 cm^2 cell culture flasks and incubated in a water jacketed incubator (Labotec, South Africa) at 37 °C and 5% CO_2 until 80 – 90 % confluency was reached.

2.4.1.3 Trypsinization of cells

Once the cells reach the desired confluency, the growth media was discarded, and the cells were washed with 3 ml of phosphate buffer saline (PBS). The PBS was discarded, and 3 ml of Trypsin (2X) was added to the flasks which were then incubated at 37 °C for 3 min. Media was added to the flasks to inactivate trypsin and the cells were collected by centrifugation at 3 000 x*g* for 3 min.

2.4.1.4 Cryopreservation of cells

For long term storage, confluent cells were trypsinized as described in section 2.4.1.3 and harvested by centrifugation at 3 000 x*g* for 3 min. The cell pellet was resuspended in 10 ml of the appropriate growth media containing 10% Dimethyl Sulfoxide (DMSO). The latter was aliquoted into 2 ml cryovial tubes and stored at -150 °C.

2.4.1.5 Total protein extraction from cell lysates

Total protein was extracted from cells using RIPA buffer according to the following protocol (Holden and Horton, 2009): once the cells reached 80 – 90 % confluency; the culture medium was removed from the cells and the cells were washed twice with cold PBS. A volume of 500 µl cold RIPA buffer was added to the cells and incubated on ice for 5min to lyse the cells. The cells were then gently scraped off the surface of the flask and the cell lysate was transferred to a microcentrifuge tube and centrifuged at 14 000 x*g* for 15 min to pellet the cell debris. The supernatant was transferred into sterile 1.5 ml microcentrifuge tubes and stored at -20 °C until further analysis.

2.4.1.6 Acetone precipitation of proteins from cell culture supernatant

Cells were cultured in 25 cm^2 cell culture flasks in the appropriate medium until about 80% confluent (about 80% of the surface of the flask is covered with cells).

Fresh growth medium was added to the cells and the cells were cultured for a further. After 24 hrs 5 ml of cell culture medium (i.e., the medium in which the cells were growing) was transferred to a sterile 50 ml tube. Cold (- 20°C) acetone (20 ml) was added to the media and the solution was vortexed for 15 seconds. The samples were incubated at - 20°C for 2 hours. Thereafter, the samples were centrifuged at 14 000 x*g* for 4 min and the supernatant was discarded. The pellet was washed twice with a 25% solution (in distilled water) of cold acetone followed by centrifugation at 14 000 x*g* for 10 min, following which the supernatant was discarded. The pellet was airdried and stored at -20°C until further analysis.

2.4.1.7 Protein quantification

The concentrations of the proteins in the cell lysates and supernatants were quantified using the Qubit® Protein Assay kit as per the manufacturer's guidelines. A Qubit® working solution was prepared by mixing 5 µl Qubit® Reagent and 195 µl of Qubit™ Buffer. Two standards (Qubit® Protein Standard #1 and Standard #2) were prepared in microcentrifuge tubes by mixing 10 µl of each Qubit® Protein Standard and 190 µl Qubit® working solution. The cell lysates and supernatant samples (10 µl) were also mixed with 190 µl Qubit® working solution. All tubes were vortexed for 3 seconds followed by a 15 min incubation period at 25 °C. The protein concentration was measured using the Qubit® 2.0 Fluorometer (Invitrogen) and the readings were recorded.

2.4.2 Analysis of cell lysates and supernatants by gel electrophoresis

2.4.2.1 SDS-PAGE analysis

The protein samples were removed from –20 °C and left to thaw on ice. Protein samples were mixed 1:1 with 2X sample buffer in sterile tubes and boiled at 95 °C in a block heater (Stuart Scientific, UK) for 5 min. Samples were removed from the hot plate and immediately placed on ice; the samples were centrifuged at 16 000 x*g* for 1 min.

Equal concentrations of each sample were loaded onto a 12% SDS-polyacrylamide gel. The gel was electrophoresed at 110 V until the Coomassie dye front reached the bottom of the gel.

2.4.2.2 Coomassie staining

After electrophoresis, the gels were removed from the plates and stained with Coomassie blue staining solution by covering the gel with Staining solution and slowly shaking it at 25 °C for 1 hour on a shaker (Belly dancer, Stovall Life Science, USA). The staining solution was then removed, the gels were rinsed with distilled water, covered in de-staining solution and slowly shaking the gels until protein bands were clearly visible on the gels. The gels were viewed and captured with a UVP Biomaging system (Upland, CA, USA).

2.4.3 Enzyme Linked Immunosorbent Assay (ELISA)

2.4.3.1 Reagent preparation

Quantitative analysis of ULBP-2 content within cell lysates and supernatants was carried out using the Human ULBP-2 DuoSet® ELISA Development system (R&D Systems) as per the manufacturer's guidelines. All reagents were brought to room temperature (25 °C) and diluted to working concentrations before use. Mouse Anti-Human ULBP-2 capture antibody was diluted to 4 µg/ml in PBS. Biotinylated Goat Anti-Human ULBP-2 detection antibody was diluted to 200 ng/ml in Reagent Diluent (1% BSA in PBS, pH 7.2-7.4, filtered with 0.2 µm). Recombinant Human ULBP-2 standard was diluted to 100 ng/ml in Reagent Diluent, and the streptavidin-HRP was diluted 1:200 in Reagent Diluent.

2.4.3.2 Plate preparation

A volume of 100 µl of the ULBP-2 capture antibody (4 µg/ml) was added per well in a 96-well microplate. The plate was sealed and incubated at 25 °C overnight.

The contents of the wells were discarded, and the wells were washed 3 times with 400 µl of the Wash Buffer (0.05% Tween®20 in PBS, pH 7.2-7.4). The non-specific binding sites of the ULBP-2 capture antibody was blocked by adding 300 µl of Reagent Diluent (1% BSA in PBS, pH 7.2-7.4, filtered with 0.2 µm) into each well and the plate incubated at 25 °C for 1 hour. The contents of the wells were discarded, and the wells were washed 3 times with the Wash Buffer.

2.4.3.3 Sandwich ELISA

A volume of 100 µl of the test sample was added to each well after which the plate was sealed and incubated at 25 °C for 2 hours. The contents of the wells were discarded, and the wells were washed 3 times with Wash Buffer. A volume of 100 µl of the biotinylated ULBP-2 detection antibody (200 ng/ml) was then added to each well. The plate was sealed and incubated at 25 °C for 2 hours. The wells were then washed 3 times with Wash Buffer. A volume of 100 µl of Streptavidin-HRP (1:200) was added to each well and the plate was sealed and incubated at 25 °C for 20 min in the dark. The wash step was repeated as above. A volume of 100 µl of Substrate solution (1:1 Colour Reagent A, H_2O_2 and Colour Reagent B, Tetramethylbenzidine) was then added to each well and the plate was incubated at 25 °C for 20 min in the dark. A volume of 50 µl of Stop Solution was added to the wells and mixed by gently tapping the plate. The optical density was determined immediately using the POLARstar® Omega plate reader (BMG LABTECH, Offenburg, Germany) set at 450 nm and 540 nm. The reading obtained at 540 nm was subtracted from at the reference wavelength 450 nm. All wells were done in triplicate. Recombinant ULBP-2 protein (supplied with the Human ULBP-2 DuoSet® ELISA Development Kit) was used as a positive control and distilled water was used as a negative control.

Recombinant ULBP-2 protein was used to construct a seven-point standard curve. Serial dilutions (between 500 and 4000 pg/µl) of the recombinant ULBP-2 protein were prepared and an ELISA was prepared as described above. Figure 2.1 shows the standard curve which was used to estimate the concentrations of ULBP-2 protein in the lysate and culture supernatant samples.

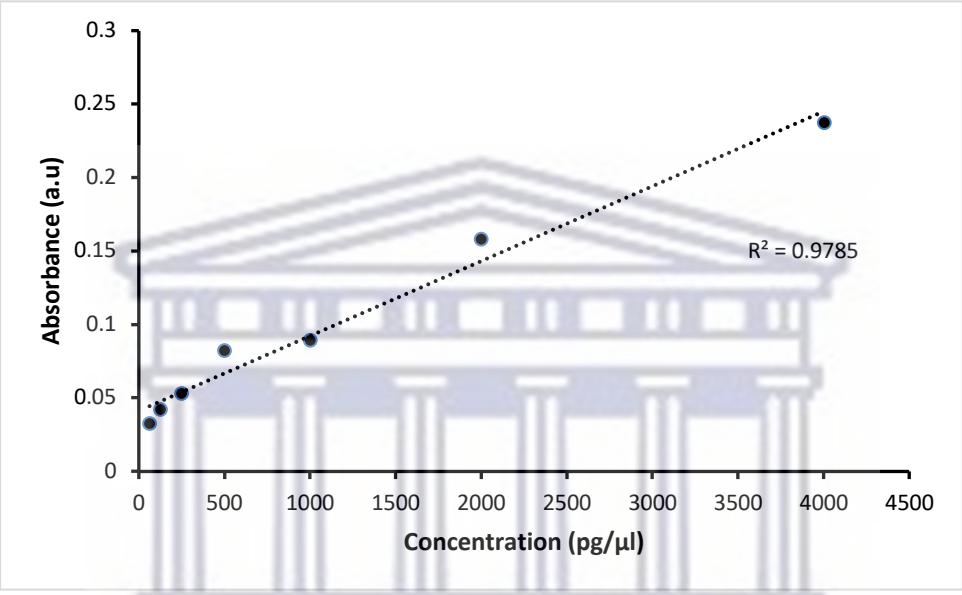

Figure 2.1: Recombinant ULBP-2 protein standard curve for ELISA. Standard curve constructed using a 2-fold dilution series of recombinant ULBP-2 protein.

2.4.4 Development of lateral flow device for detection of ULBP-2

2.4.4.1 Synthesis of 14 nm colloidal gold

Gold nanoparticles (GNPs) were synthesized using trisodium citrate ($Na_3C_6H_5O_7.2H_2O$) reduction of tetrachloroaurate ($HAuCl_4.3H_2O$) as previously described by Sosibo *et al* (2015). Distilled water was briefly brought to a boil and stirred at 660 rpm with a magnetic stirrer. A 34 mM $HAuCl_4.3H_2O$ aqueous solution was added to the water and after a few seconds, a 1% (w/v) trisodium citrate aqueous solution was poured into the beaker.

The mixture was boiled under reflux conditions until the solution changed colour from grey to deep red (approximately 7 min). The heat was switched off and the mixture was allowed to cool to room temperature for 2 hours while stirring. The optical absorption spectra (300-750nm) of the GNPs was determined using the Multiskan GO UV-Vis spectrometer (Thermo Fisher Scientific).

2.4.4.2 Characterization of GNPs by High-resolution transmission electron microscopy (HRTEM) and Dynamic light scattering (DLS)

The structure and size distribution of GNPs were analysed by HRTEM using a FEI Tecnai G2 20 field-emission HRTEM (Oregon, OR, USA) as described by Majoumouo *et al* (2020). The samples were prepared by drop-coating one drop of the GNPs onto a carbon-coated copper grid. The GNPs were dried under a Xenon lamp for 10 min and analysed by HRTEM. Transmission electron micrographs were captured in the bright field mode at an accelerating voltage of 200 KeV. The TEM micrographs were analysed using origin 8.5 and Image J Software (50b version 1.8.0_60).

The GNPs were analyzed by DLS to measure their hydrodynamic size, zeta potential and polydispersity index (PDI) using a Zetasizer (Malvern Instruments Ltd., Malvern, UK). A 1:1000 dilution was made with GNPs in distilled water and 1 ml of sample was used for analysis.

2.4.4.3 Conjugation and functionalization of GNPs

A solution of GNPs was adjusted to pH 9 using 0.2M potassium carbonate. The capture antibody, ULBP-2 antibody (R&D Systems) was reconstituted in 10mM PBS to 0.2 µg/µl. A volume of 25 µl of the antibody was added to 500 µl of GNPs in a 1.5 ml microcentrifuge tube and incubated at 23 °C for 1 hour while shaking at 500 rpm.

A volume of 100 µl of 10% NaCl was added to the tube and the tube was incubated at 25 °C for 10 min while shaking at 500 rpm. The conjugate was then centrifuged at 10 000 rpm for 5 min. The supernatant was discarded, and the pellet containing the GNP- antibody conjugates were resuspended in dH_2O. The Multiskan GO UV-Vis spectrometer was used to confirm the conjugation of the antibody to GNPs by assessing changes in optical absorption spectra.

2.4.4.4 Development of the ULBP dipstick assay

The dipstick assay also referred to as the wet test, is often used as a preliminary test towards the development of an LFA. The principle of the dipstick assay is similar to the LFA. It consists of a membrane strip (the same membrane that will be used in the development of the LFA) onto which the analyte or biomarker is immobilized as seen in Figure 2.2. The membrane is dipped into a solution containing a mixture of the test sample (which may or may not contain the analyte or biomarker molecule) and GNPs conjugated to an antibody that is specific for the analyte or biomarker. If the analyte is absent from the test sample, the GNP-antibody conjugate will migrate over the membrane strip by capillary action and bind to the immobilized analyte resulting in the formation of a signal which indicates that sample does not contain the analyte. Conversely, if the analyte is present in the test sample, the GNP-antibody conjugate will bind to the analyte forming GNP-antibody/analyte complex. The GNP-antibody/analyte complex is unable to bind to the immobilized analyte and no signal will be produced on the strip, indicating the presence of the analyte in the test sample.

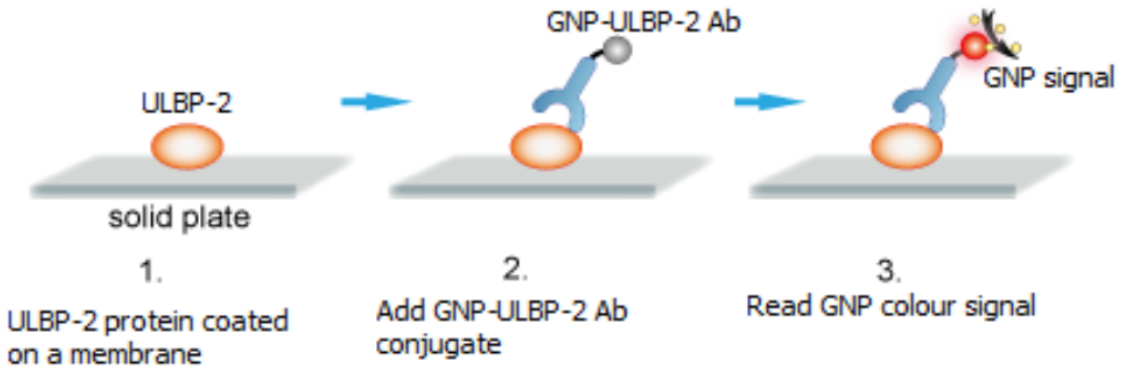

Figure 2.2: Workflow and the principle of the GNP-based LFA showing a negative result for ULBP-2 in sample. ULBP-2 is immobilized on the membrane to which GNP-ULBP-2 Antibody conjugate is added. As there is no ULBP-2 protein in the test sample, the conjugate binds to the immobilized ULBP-2 and a colour signal is visible.

Nitrocellulose membranes (DCN Diagnostics, USA) were cut into strips (8cm long and 0.5cm wide). Recombinant ULBP2 protein (10 µg) of was spotted on the membrane strip at a distance between 3 cm from the bottom of the trip. The membrane was then dried on a heating block at 37 °C for 30 minutes. The membrane was blocked with a blocking buffer (1xPBS containing 0.05mg/mL BSA) and dried on a heating block at 37 °C for 30 minutes. The strip was then tested by submerging the spotted end in a 2 mL microcentrifuge tube containing 300 µL of the GNP-ULBP-2 Ab conjugate solution. The strip was removed once after 30 min and an digital image of the strip was captured using a camera.

Chapter 3: Results and Discussion

3.1 Evaluation of ULBP-2 expression in cancer cell lysates and supernatants

A study by Yamaguchi *et al* (2012) analysed the culture supernatants of 20 lung cancer cell lines and showed that the supernatants of NSCLC cell lines, but not small-cell lung cancer (SCLC) cell lines contain ULBP-2. This suggests that NSCLC cell lines release or secrete ULBP-2. It is not known if breast cancer cell lines also release ULBP-2, but a previous study showed that ULBP-2 may be over expressed in breast cancer patients (Ngcoza, 2013). In the current study, the expression and release of ULBP-2 was investigated in 5 cancer cell lines. This included a non-cancerous breast cell line (MCF-12A), a breast cancer cell line (MCF-7), a cervical cancer (HeLa), a colorectal adenocarcinoma cell line (HT-29), and a lung cancer cell line (A549).

Cell lysates represent the intra- and extra-cellular proteins bound in the cell membranes, internal organelles or cytosolic proteins, while the culture supernatant represents released or secreted cellular proteins. Lysates and 24hr old culture supernatants were prepared for all 5 cell lines. Protein samples from the cell lysate and cell culture supernatant were resolved on a 12% SDS polyacrylamide gel. **Figures 3.1 (a) and (b)** respectively show the protein samples for the lysates and culture supernatants extracted from the 5 cell lines. Several protein bands with sizes varying between less than 14 and 116 kDa were observed for the lysates and culture supernatants. The band patterns of the proteins were very distinct for each cell line and the band pattern of the lysates and culture supernatants were also very different.

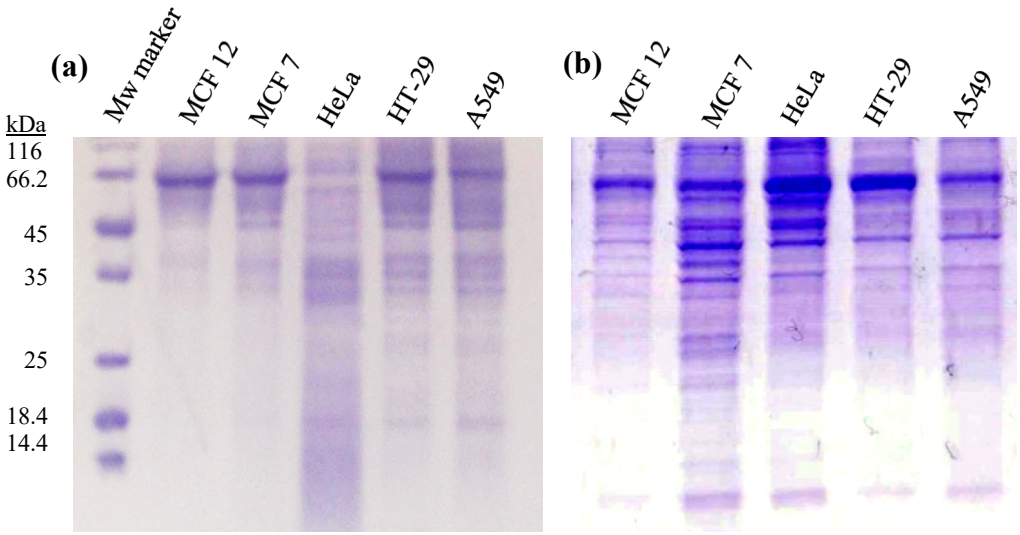

Figure 3.1. Expression of ULBP-2 in cell lysates and supernatant of various cell lines. Protein samples were separated on a 12% polyacrylamide gel stained with Coomassie blue. **(a)** Total protein from cell culture supernatants and **(b)** cell lysates of five different cell lines cultured in FBS-free media.

ELISA was used to assess if ULBP-2 was present in the cell lysates and cell culture supernatants of the various cell lines. ELISA is based on antigen-antibody binding, and therefore provides more specificity and sensitivity for the detection of analytes in complex mixtures (Chen *et al.,* 2019).

The results of the ELISA (**Figure 3.2.a**) showed that the lysates of the 5 cell lines did not contain ULBP2 since the absorbance readings obtained for the cell lines were not significantly different from the negative control. The absorbance readings obtained for the culture supernatants of MCF-12A, MCF-7, HT-29, and A549 (**Figure 3.2.b**) were also not significantly different from the negative control suggesting that these samples also did not contain ULBP-2. However, at 0.75 the absorbance readings for the culture supernatant for HeLa cells were significantly higher than the negative control and the other cell lines. In fact, the absorbance reading was similar to that of the positive control which contained 100 ng/ml of recombinant ULPB-2 protein.

This suggests that amongst these 5 cell lines, the cervical cancer cell line, HeLa was the only cell line that releases or secretes ULBP-2. Unfortunately, the standard curve was not suitable to determine the concentration of ULBP-2 in the HeLa culture supernatant, as the highest concentration of recombinant ULPB-2 protein used to produce the standard curve had an absorbance reading of only 0.23, while the absorbance value for the HeLa culture supernatant was 0.75 and therefore out of range for the standard curve. However, the concentration of ULPB-2 in this sample is higher than 4000 pg/µl. While this study started out looking to confirm that breast cancer cells secrete or release ULBP-2, it was found that the breast cancer cell line, MCF7 used in this study did not express ULBP-2 and did not release this protein into the culture supernatant. However, it was shown that cervical cancer cell line HeLa secreted or released ULBP-2. The release of ULBP-2 seemed to be cell line specific and may therefore also be cancer specific. This is in line with the findings of the study Yamaguchi *et al* (2012), which found that NSCLC cell lines, but not SCLC release ULBP2. The Bioinformatics study which suggested that ULBP-2 may be over expressed in breast cancers was performed on microarray data generated from tissue obtained from breast cancer patients. The MCF7 cell line used in the current study was derived from the breast tissue of a patient with metastatic adenocarcinoma. It is possible that the expression of ULBP-2 in this breast cancer cell is low.

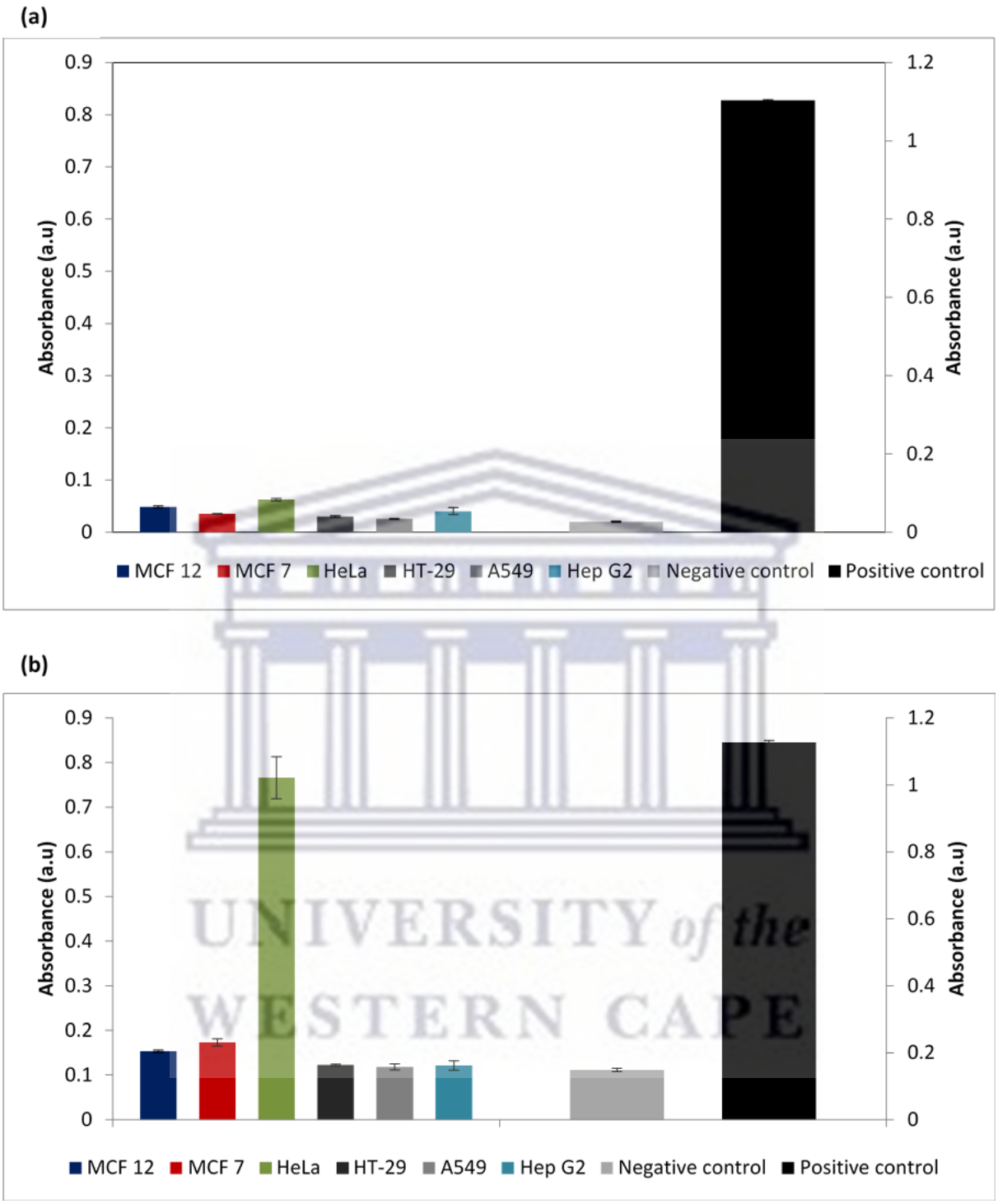

Figure 3.2: Evaluation of ULBP-2 expression by ELISA. Cell lysates (a) and cell culture supernatants (b) of a non-cancer and different cancer cell lines. Negative control – dH_2O, Positive control - recombinant ULBP-2 protein.

3.2 Development of GNP-based LFA for detection of ULBP-2

GNP-based LFAs are convenient diagnostic tools for POC testing. They are cost effective, rapid, and user friendly, which makes them ideal for screening tests. Nanomaterials have gained much interest in medicine due to the unique properties conferred to them by their increased surface to volume ratio with some displaying improved mechanical, electronic, photo or magnetic properties compared to their bulk counterparts (Ramos *et al.,* 2017). GNPs in particular have favourable optical properties for use in diagnostic applications and exhibit good size-dependent optical resonance. Photoactivation of GNPs results in significant enhancement of its electromagnetic field, causing the scattering and absorption of light. This can be exploited to generate colour change or heat, making GNPs ideal detection components for diagnostic systems and biosensors (Caracciolo *et al.,* 2019). One can also measure the shift of light absorption generated by the conjugation of GNPs to their targets. Notably, the use of GNPs within this context offers some unique advantages compared to the use of fluorescent dyes since they avoid photodecomposition, they are biocompatible, and most significantly they demonstrate a very precise correlation of their chemical/physical properties to their optical characteristics, which if accurately measured can confer improved minimum detection limit and sensitivity (Singh *et al.,* 2018).

3.2.1 Synthesis and characterisation of GNPs

GNPs with a diameter of 14 nm were synthesised using the citrate reduction method described by Sosibo *et al* (2015). The surface morphology and physico-chemical characteristics of synthesized GNPs were studied via HR-TEM, UV-Vis Spectroscopy and DLS. The HR-TEM micrograph in **Figure 3.3 (a)** shows monodispersed and spherical GNPs with an average core diameter of 14 ± 5nm. DLS was used to further study the hydrodynamic size of the GNPs which showed average particle size of 36.48 nm in **Figure 3.4 (b)**. The average particle size measured by DLS was larger (36 nm) than determined by TEM analysis (14 nm).

The difference in the size of the GNPs between the two methods is due to the different principles of each method. With TEM, particles are examined in a dried state and will appear smaller than with DLS, where the particles are examined in solution. This is due to ionic species in the solution that interact with and surround the particles, thus increasing their hydrodynamic size (Inam *et al.,* 2022).

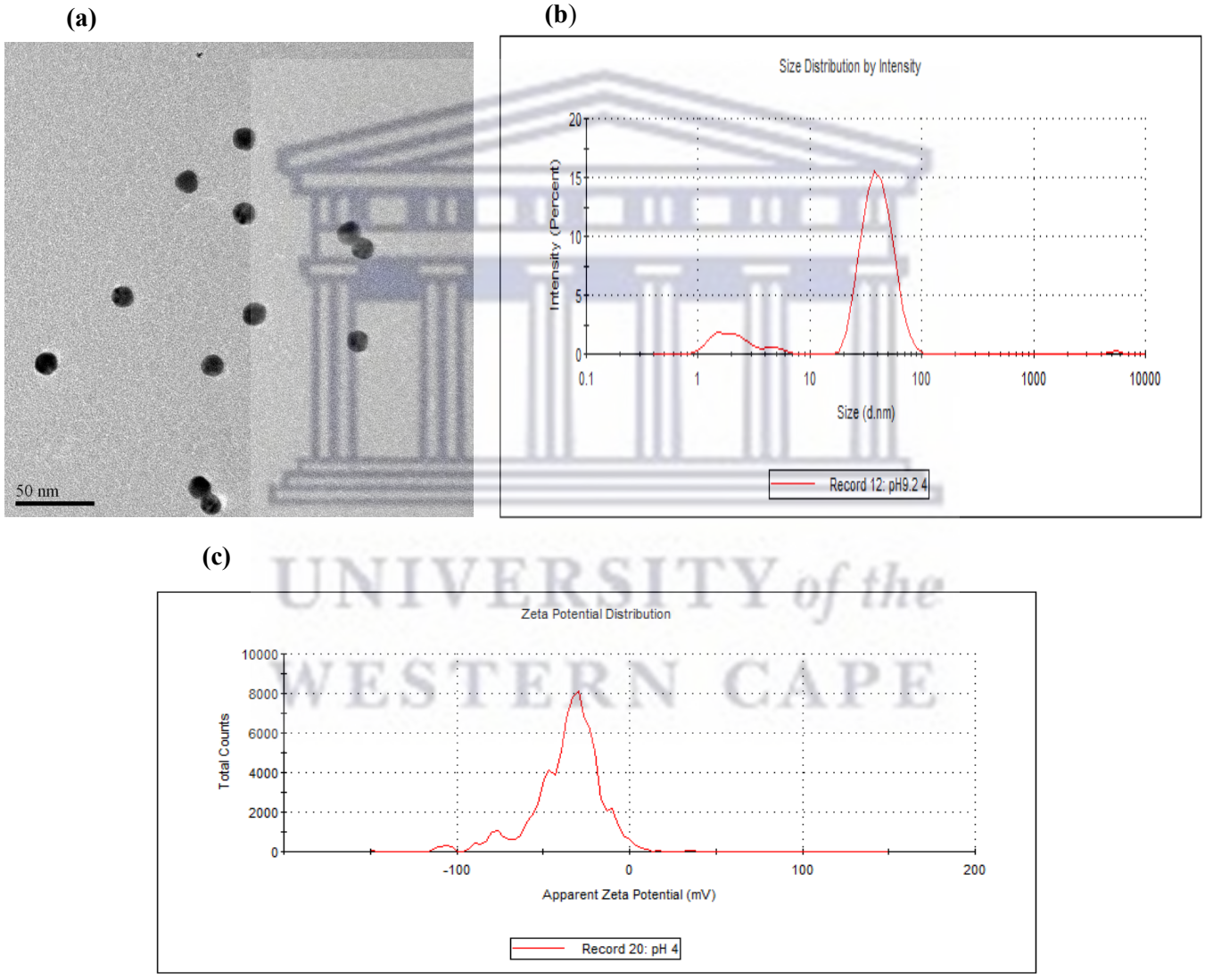

Figure 3.3: Characterization of GNPs. HR-TEM image of colloidal gold particles (a), DLS analysis of Z-average particle size (b), and zeta potential (c).

According to Danaei *et al* (2018) PDI values above 0.7 indicate that the sample has a very broad particle size distribution. Since the PDI of the GNPs produced in this study was 0.357, it can be concluded that the GNPs have a uniform distribution.

DLS was also used to study the surface charge of GNPs at pH 9 in **Figure 3.4 (c)**, which showed a zeta potential of -36.2mV. This indicated that GNPs are moderately stable in pH 9 solution.

GNPs absorb light in the visible range (500 nm-600 nm), and this can be measured by UV-vis spectroscopy. UV-vis spectroscopy can therefore be used to characterise GNPs. Lambda max, i.e., the wavelength at which the GNPs have their strongest photon absorption, increases with the size of the GNPs. Changes on the surface of GNPs, such as the binding of an antibody to the GNPs or the binding of GNPs to each other (i.e., GNP aggregation) can result in changes in the UV-vis spectra, in particular lambda max. Changes in the UV-vis spectra can also be observed as changes in the colour of a GNP solution. This property of GNPs can be used to test the stability of the GNPs. It can also be used in biosensing and the development of diagnostic assays to detect the presence of biomolecules such as biomarker proteins.

The GNPs synthesised in this study were analysed by UV-vis spectroscopy. The peak absorbance or lambda max for the GNPs synthesised in this study was 530 nm and is therefore within the absorption spectrum expected for GNPs. The stability of the GNPs at different pH conditions was determined by resuspending the GNPs in PBS with a pH range of 5 to 9. The GNPs had a native pH of 5 after synthesis. **Figure 3.4** shows the UV-vis spectra of the GNPs as the pH of the solution increases from pH 5 to 9. Measurements were taken at pH 5, 8, 8.5 and 9. **Figure 3.4** shows that lambda max (530nm) did not change at the different pH conditions, which suggest that the GNPs were stable at all these conditions.

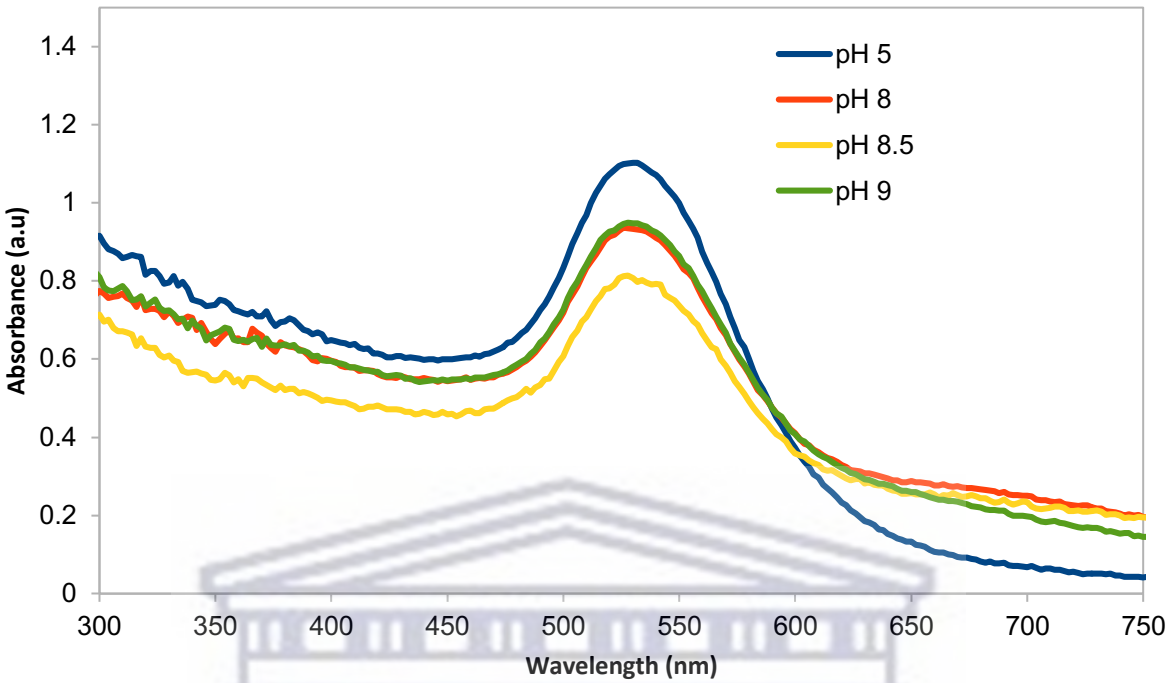

Figure 3.4: UV-Vis spectra of GNPs under different pH conditions.

The GNPs were incubated with increasing concentrations (8, 10, and 12 µg/ml) of the ULBP-2 antibody, and upon addition of the NaCl to the conjugate, changes were observed in their UV-vis spectra as shown in **Figure 3.6**. Significant changes occurred when ULBP-2 antibody concentrations ≥ 10 µg/ml were used, at 12 µg/ml the GNPs changed colour to purple to indicate their aggregation which was confirmed by their UV-vis spectra. The lowest concentration of ULBP-2 antibody i.e., 8 µg/ml yielded the curve most similar to the one for the GNP alone and was therefore selected as the concentration for the development of the GNP-based ULBP-2 LFA. This suggests that at 8 µg/ml, the ULBP-2 antibody is conjugated to the GNPs without causing the aggregation of the GNPs. Higher concentrations of the GNPs appear to result in the aggregation of the GNPs.

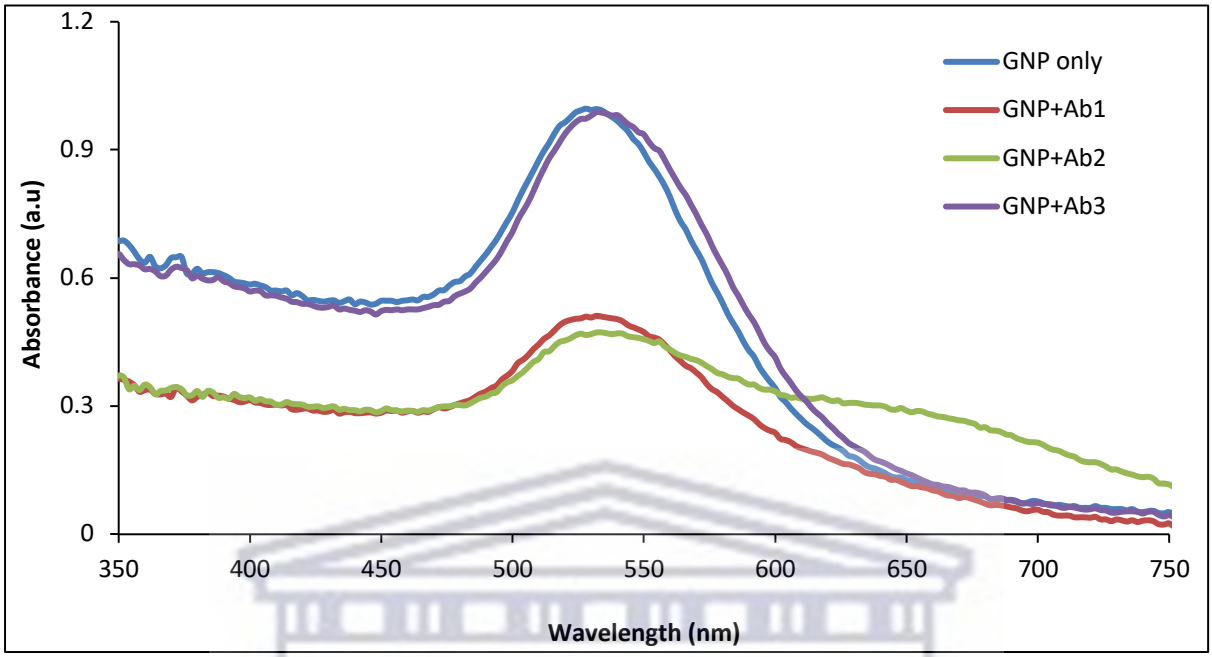

Figure 3.5: UV-vis spectra of GNPs following conjugation to ULBP-2 antibody. Ab1 = 12µg/ml, Ab2 = 10µg/ml, Ab3 = 8µg/ml, GNP only = GNP without Ab. Lambda max for GNP only, GNP+Ab1, GNP+Ab2 and GNP+Ab3, was 530, 530, 534 and 540nm, respectively.

3.2.2 Changes in the UV-vis spectra of GNP-ULBP-2 conjugate in the presence of the lysate and culture supernatant

The feasibility of using the GNPs-ULBP-2 antibody conjugated in a LFA was tested using the lysate and culture supernatant from HeLa cells. The ELISA (**Figure 2.2**) showed that the culture supernatant contained ULBP-2, but that the lysate did not. The GNPs-ULBP-2 antibody conjugated was incubated with the cell lysate (Target 1) and cell culture supernatant (Target 2), and subsequently subjected to UV-vis spectroscopy. Lambda max for GNP-ULBP-2 in the presence of the cell lysate and GNP-ULBP-2 in the presence of the culture supernatant increased to 542nm from 534nm (GNP-ULBP-2) (**Figure 3.6**). The shape of the spectra was also wider compared to the spectrum obtained for GNP-ULBP-2.

This suggests that the surface of the GNP-ULBP-2 changed in the presence of both the cell lysate and culture supernatant, but that both the cell lysate and culture supernatant affected GNP-ULBP-2 in the same way.

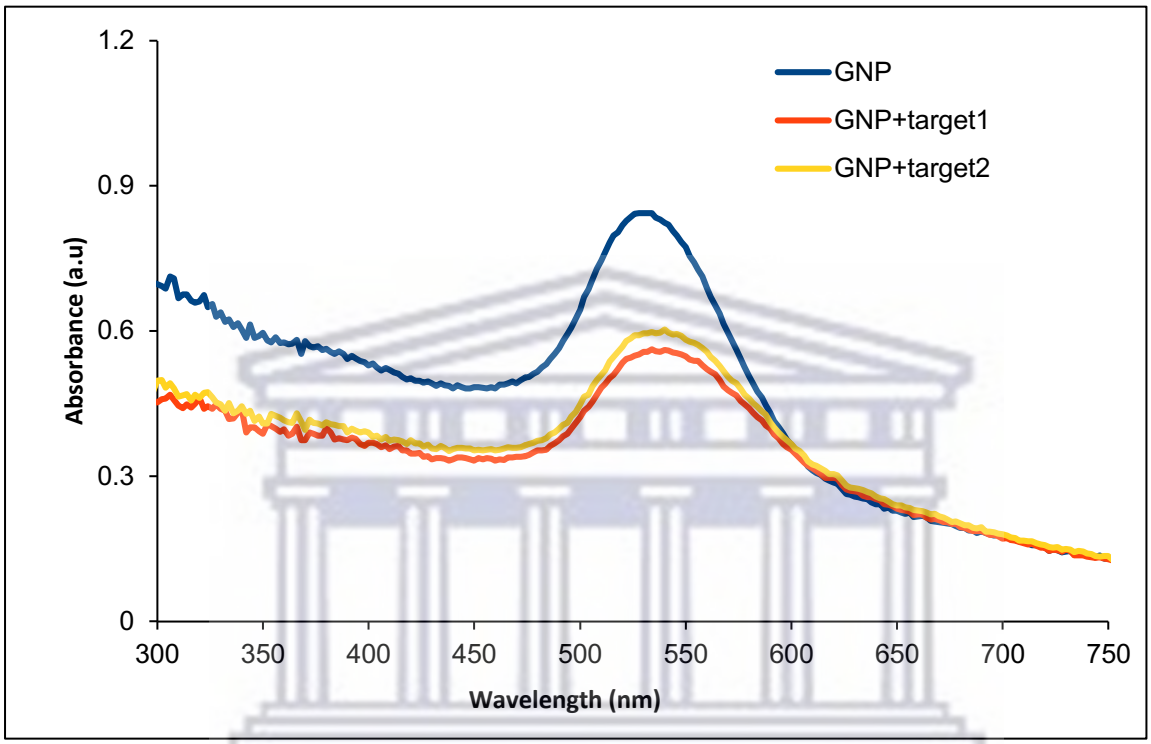

Figure 3.6: GNPs with target protein obtained from HeLa cells. Target1 = cell lysate; Target2 = cell culture supernatants.

3.2.3 Testing the ULBP dipstick assay

The ULBP-2 dipstick assay was tested to ascertain if the GNP-ULBP-2 antibody conjugate will be able to bind to recombinant ULBP-2 protein immobilized on a membrane. **Figure 3.7** shows the result of this test. A positive result would be indicated by the formation of a dot in the area where the protein was spotted. Instead, **Figure 3.7** shows a blank spot surrounded by a dark outer layer in the area where the recombinant ULBP-2 protein was spotted.

However, this result suggests that the GNP-ULBP-2 antibody conjugate was bound to the recombinant ULBP-2 protein immobilized on the membrane and that the GNP-ULBP-2 antibody conjugate can be applied in a LFA to detect ULBP-2 protein in a test sample. The blank area in the middle of the spot is likely due to the high concentration of the recombinant ULBP-2 protein immobilised on the strip. This is similar to the phenomenon that is observed with western blot analysis when so called "ghost bands" appear on the blot when the concentration of the antibody used to detect the target protein on the membrane is too high or too much of the protein was transferred onto the membrane (Alegria-Schaffer *et al.,* 2009). Because the concentration of recombinant ULBP-2 protein immobilized on the membrane is very high in the middle of the spot and lower at the edges of the spot, only the outer edges of the protein spot was visible.

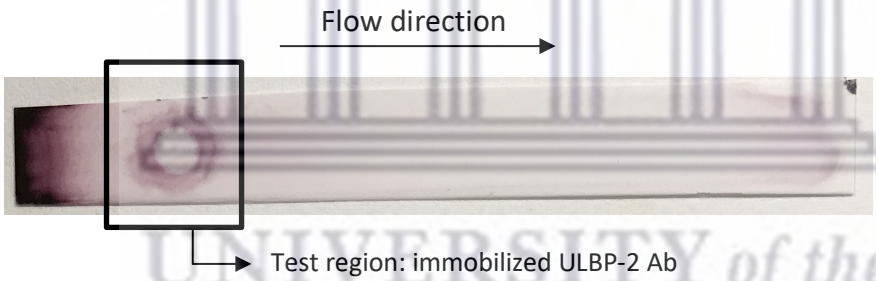

Figure 3.7: Detection of recombinant ULBP-2 using the dipstick assay. Recombinant ULBP-2 protein was spotted in the area indicated by the black square. A solution of GNP-ULBP-2 antibody conjugate was allowed to migrate over the membrane in the direction of the arrow.

Chapter 4: Conclusion

The aims of this study were to investigate the expression of ULBP-2 in a panel of cancer cell lines and to develop a lateral flow assay to detect this protein. Based on prior knowledge ULBP-2 is possibly a biomarker for breast cancer and is possibly also secreted or released by cancer cells. The expression of ULBP-2 in the cell lysates and culture supernatants of 5 cell lines which included a breast cancer cell line (MCF7), and a non-cancerous breast cell line (MCF 12A) was investigated using ELISA. This study found that neither of these breast cell lines express ULBP-2. However, the cervical cancer cell line, HeLa was the only cell line that secreted or released ULBP-2 into the culture supernatant. This study could not confirm whether ULBP-2 is a biomarker for breast cancer. However, the literature suggests the overexpression of this biomarker protein may be cancer specific. This is also supported by the findings of the current study. Hence different breast cancer cell lines should be evaluated in the future. The fact that ULBP-2 appears in the culture supernatant makes it a highly suitable target for the development of a less invasive cancer diagnostic assay. Literature suggests that in some cancers, ULBP-2 is present in the sera of cancer patients. This means that diagnosis or cancer screening can be performed from a blood sample, which is much less invasive than using a tissue biopsy sample. GNPs of 14nm diameter were synthesised and successfully conjugated to a ULBP-2 antibody. GNP-ULBP-2 conjugate was used to develop a dipstick assay for the detection of ULBP-2 protein. This study demonstrated the application of the dipstick assay to detect recombinant ULBP-2 protein. While this assay is not an LFA, it demonstrates that it is feasible to develop a LFA for the detection of ULBP-2, a soluble potential biomarker protein for some cancers.

Future work should include evaluating the dipstick assay in the presence of free ULBP-2 protein i.e., a control experiment where the GNP-ULBP-2 conjugate is mixed with recombinant ULBP-2, prior to dipping the membrane strip in the sample. This will be representative of a positive test result. The next step would be to evaluate the assay on a more complex sample, such as culture supernatant and thereafter, develop a sandwich format LFA. This assay can potentially be used as a cost-effective cancer screening tool.

References

Agersborg, S., Mixon, C., Nguyen, T., Aithal, S., Sudarsanam, S., Blocker, F., Weiss, L., Gasparini, R., Jiang, S., Chen, W. and Hess, G., 2018. Immunohistochemistry and alternative FISH testing in breast cancer with HER2 equivocal amplification. *Breast Cancer Research and Treatment*, *170*(2), pp.321-328.

Aguilar-Cazares, D., Chavez-Dominguez, R., Carlos-Reyes, A., Lopez-Camarillo, C., Hernadez de la Cruz, O.N. and Lopez-Gonzalez, J.S., 2019. Contribution of angiogenesis to inflammation and cancer. *Frontiers in oncology*, *9*, p.1399.

Ahn, S., Woo, J.W., Lee, K. and Park, S.Y., 2020. HER2 status in breast cancer: changes in guidelines and complicating factors for interpretation. *Journal of pathology and translational medicine*, *54*(1), pp.34-44.

Ahn, S., Woo, J.W., Lee, K. and Park, S.Y., 2020. HER2 status in breast cancer: changes in guidelines and complicating factors for interpretation. *Journal of pathology and translational medicine*, *54*(1), pp.34-44.

Alegria-Schaffer, A., Lodge, A. and Vattem, K., 2009. Performing and optimizing Western blots with an emphasis on chemiluminescent detection. *Methods in enzymology*, *463*, pp.573-599.

Barzaman, K., Karami, J., Zarei, Z., Hosseinzadeh, A., Kazemi, M.H., Moradi-Kalbolandi, S., Safari, E. and Farahmand, L., 2020. Breast cancer: Biology, biomarkers, and treatments. *International immunopharmacology*, *84*, p.106535.

Bickelhaupt, S., Paech, D., Kickingereder, P., Steudle, F., Lederer, W., Daniel, H., Götz, M., Gählert, N., Tichy, D., Wiesenfarth, M. and Laun, F.B., 2017. Prediction of malignancy by a radiomic signature from contrast agent-free diffusion MRI in suspicious breast lesions found on screening mammography. *Journal of magnetic resonance imaging*, *46*(2), pp.604-616.

Boehringer, H.R. and O'Farrell, B.J., 2022. Lateral flow assays in infectious disease diagnosis. *Clinical Chemistry*, *68*(1), pp.52-58.

Bogdanovska-Todorovska, M., Petrushevska, G., Janevska, V., Spasevska, L. and Kostadinova-Kunovska, S., 2018. Standardization and optimization of fluorescence in situ hybridization (FISH) for HER-2 assessment in breast cancer: A single center experience. *Bosnian journal of basic medical sciences*, *18*(2), p.132.

Caracciolo, G., Vali, H., Moore, A. and Mahmoudi, M., 2019. Challenges in molecular diagnostic research in cancer nanotechnology. *Nano Today*, *27*, pp.6-10.

Chen, L., Ruan, F., Sun, Y., Chen, H., Liu, M., Zhou, J. and Qin, K., 2019. Establishment of sandwich ELISA for detecting the H7 subtype influenza A virus. *Journal of Medical Virology*, *91*(6), pp.1168-1171.

Chen, X., Leng, Y., Hao, L., Duan, H., Yuan, J., Zhang, W., Huang, X. and Xiong, Y., 2020. Self-assembled colloidal gold superparticles to enhance the sensitivity of lateral flow immunoassays with sandwich format. *Theranostics*, *10*(8), p.3737.

Christensen-Jeffries, K., Couture, O., Dayton, P.A., Eldar, Y.C., Hynynen, K., Kiessling, F., O'Reilly, M., Pinton, G.F., Schmitz, G., Tang, M.X. and Tanter, M., 2020. Super-resolution ultrasound imaging. *Ultrasound in medicine & biology*, *46*(4), pp.865-891.

Corso, G., Figueiredo, J., De Angelis, S.P., Corso, F., Girardi, A., Pereira, J., Seruca, R., Bonanni, B., Carneiro, P., Pravettoni, G. and Guerini Rocco, E., 2020. E-cadherin deregulation in breast cancer. *Journal of Cellular and Molecular Medicine*, *24*(11), pp.5930-5936.

Danaei, M., Dehghankhold, M., Ataei, S., Hasanzadeh Davarani, F., Javanmard, R., Dokhani, A., Khorasani, S. and Mozafari, M.R., 2018. Impact of particle size and polydispersity index on the clinical applications of lipidic nanocarrier systems. *Pharmaceutics*, *10*(2), p.57.

Dange, V.N., Shid, S.J., Magdum, C.S. and Mohite, S.K., 2017. A Review on Breast cancer: An Overview. *Asian Journal of Pharmaceutical Research*, *7*(1), pp.49-51.

Demirkol, S., Gomceli, I., Isbilen, M., Dayanc, B.E., Tez, M., Bostanci, E.B., Turhan, N., Akoglu, M., Ozyerli, E., Durdu, S. and Konu, O., 2017. A combined ULBP2 and SEMA5A expression signature as a prognostic and predictive biomarker for colon cancer. *Journal of Cancer*, *8*(7), p.1113.

Deng, J.L., Xu, Y.H. and Wang, G., 2019. Identification of potential crucial genes and key pathways in breast cancer using bioinformatic analysis. *Frontiers in Genetics*, *10*, p.695.

Dhar, P. and Wu, J.D., 2018. NKG2D and its ligands in cancer. *Current opinion in immunology*, *51*, pp.55-61.

Ding, H., Yang, X. and Wei, Y., 2018. Fusion proteins of NKG2D/NKG2DL in cancer immunotherapy. *International Journal of Molecular Sciences*, *19*(1), p.177.

Echle, A., Rindtorff, N.T., Brinker, T.J., Luedde, T., Pearson, A.T. and Kather, J.N., 2021. Deep learning in cancer pathology: a new generation of clinical biomarkers. *British journal of cancer*, *124*(4), pp.686-696.

Feng, Y., Spezia, M., Huang, S., Yuan, C., Zeng, Z., Zhang, L., Ji, X., Liu, W., Huang, B., Luo, W. and Liu, B., 2018. Breast cancer development and progression: Risk factors, cancer stem cells, signaling pathways, genomics, and molecular pathogenesis. *Genes & diseases*, *5*(2), pp.77-106.

Ferlay, J., Colombet, M., Soerjomataram, I., Parkin, D.M., Piñeros, M., Znaor, A. and Bray, F., 2021. Cancer statistics for the year 2020: An overview. *International journal of cancer*, *149*(4), pp.778-789.

Foroughi, S., Tie, J., Gibbs, P. and Burgess, A.W., 2019. Epidermal growth factor receptor ligands: Targets for optimizing treatment of metastatic colorectal cancer. *Growth Factors*, *37*(5-6), pp.209-225.

Frazao, A., Rethacker, L., Messaoudene, M., Avril, M.F., Toubert, A., Dulphy, N. and Caignard, A., 2019. NKG2D/NKG2-ligand pathway offers new opportunities in cancer treatment. *Frontiers in Immunology*, *10*, p.661.

Geisel, J., Raghu, M. and Hooley, R., 2018, February. The role of ultrasound in breast cancer screening: the case for and against ultrasound. In *Seminars in Ultrasound, CT and MRI*(Vol. 39, No. 1, pp. 25-34). WB Saunders.

Georgakopoulos-Soares, I., Chartoumpekis, D.V., Kyriazopoulou, V. and Zaravinos, A., 2020. EMT factors and metabolic pathways in cancer. *Frontiers in oncology*, *10*, p.499.

Gilbert, F.J. and Pinker-Domenig, K., 2019. Diagnosis and staging of breast cancer: when and how to use mammography, tomosynthesis, ultrasound, contrast-enhanced mammography, and magnetic resonance imaging. *Diseases of the Chest, Breast, Heart and Vessels 2019-2022*, pp.155-166.

Han, Y., Xie, W., Song, D.G. and Powell, D.J., 2018. Control of triple-negative breast cancer using ex vivo self-enriched, costimulated NKG2D CAR T cells. *Journal of hematology & oncology*, *11*(1), pp.1-13.

Hanahan D, Weinberg R. A., 2011. Hallmarks of cancer: the next generation. Cell. ;144(5):646-74. doi: 10.1016/j.cell.2011.02.013. PMID: 21376230.

Hassanpour, S.H. and Dehghani, M., 2017. Review of cancer from perspective of molecular. *Journal of Cancer Research and Practice*, *4*(4), pp.127-129.

Holden, P. and Horton, W.A., 2009. Crude subcellular fractionation of cultured mammalian cell lines. *BMC research notes*, *2*(1), pp.1-10.

Huber, D., von Voithenberg, L.V. and Kaigala, G.V., 2018. Fluorescence in situ hybridization (FISH): History, limitations and what to expect from micro-scale FISH?. *Micro and Nano Engineering*, *1*, pp.15-24.

Imran, A., Qamar, H.Y., Qurban, A.L.I., Naeem, H., Mariam, R.I.A.Z., Saima, A.M.I.N., Kanwal, N., Fawad, A.L.I., Sabar, M.F. and Nasir, I.A., 2017. Role of molecular biology in cancer treatment: A review article. *Iranian journal of public health*, *46*(11), p.1475.

Inam, W., Bhadane, R., Akpolat, R.N., Taiseer, R.A., Filippov, S.K., Salo-Ahen, O.M., Rosenholm, J.M. and Zhang, H., 2022. Interactions between polymeric nanoparticles and different buffers as investigated by zeta potential measurements and molecular dynamics simulations. *View*, *3*(4), p.20210009.

Jafari, S.H., Saadatpour, Z., Salmaninejad, A., Momeni, F., Mokhtari, M., Nahand, J.S., Rahmati, M., Mirzaei, H. and Kianmehr, M., 2018. Breast cancer diagnosis: Imaging techniques and biochemical markers. *Journal of cellular physiology*, *233*(7), pp.5200-5213.

Jayanthi, V.S.A., Das, A.B. and Saxena, U., 2017. Recent advances in biosensor development for the detection of cancer biomarkers. *Biosensors and Bioelectronics*, *91*, pp.15-23.

Jeong, S., Park, M.J., Song, W. and Kim, H.S., 2020. Current immunoassay methods and their applications to clinically used biomarkers of breast cancer. *Clinical biochemistry*, *78*, pp.43-57.

Jørgensen, J.T. and Winther, H., 2019. The Development of the HercepTest™—from Bench to Bedside. *Molecular Diagnostics*, pp.43-60.

Kegasawa, T., Tatsumi, T., Yoshioka, T., Suda, T., Ikezawa, K., Nakabori, T., Yamada, R., Kodama, T., Shigekawa, M., Hikita, H. and Sakamori, R., 2019. Soluble UL16-binding protein 2 is associated with a poor prognosis in pancreatic cancer patients. *Biochemical and Biophysical Research Communications*, *517*(1), pp.84-88.

Koczula KM, Gallotta A. Lateral flow assays. Essays Biochem. 2016 Jun 30;60(1):111-20. doi: 10.1042/EBC20150012. PMID: 27365041; PMCID: PMC4986465.

Leinco Technologies, 2022. Methods and Principles from our Scientific Staff. Available at: https://www.leinco.com/sandwich-elisa-protocol/ (Accessed: 11 June 2022)

Li, K., Chen, Y., Li, A., Tan, C. and Liu, X., 2019. Exosomes play roles in sequential processes of tumor metastasis. *International journal of cancer*, *144*(7), pp.1486-1495.

Li, N., Cui, J., Wen, C. and Huang, K., 2020. Different cellular properties and loss of nuclear signalling of porcine epidermal growth factor receptor with aging. *General and Comparative Endocrinology*, *290*, p.113415.

Li, Y., Liu, L., Xu, C., Kuang, H. and Sun, L., 2021. Integration of antibody-antigen and receptor-ligand reactions to establish a gold strip biosensor for detection of 33 β-lactam antibiotics. *Science China Materials*, *64*(8), pp.2056-2066.

Liu, W., Liu, X., Liu, C., Zhang, Z. and Jin, W., 2020. Development of a sensitive monoclonal antibody-based sandwich ELISA to detect Vip3Aa in genetically modified crops. *Biotechnology Letters*, *42*(8), pp.1467-1478.

Liu, X., Zheng, W., Wang, W., Shen, H., Liu, L., Lou, W., Wang, X. and Yang, P., 2017. A new panel of pancreatic cancer biomarkers discovered using a mass spectrometry-based pipeline. *British journal of cancer*, *117*(12), pp.1846-1854.

Loibl, S. and Gianni, L., 2017. HER2-positive breast cancer. *The Lancet*, *389*(10087), pp.2415-2429.

Maciejowski, J. and de Lange, T., 2017. Telomeres in cancer: tumour suppression and genome instability. *Nature reviews Molecular cell biology*, *18*(3), pp.175-186.

Madhukumar, S., Thambiran, U.R., Basavaraju, B. and Bedadala, M.R., 2017. A study on awareness about breast carcinoma and practice of breast self-examination among basic sciences' college students, Bengaluru. *Journal of family medicine and primary care*, *6*(3), p.487.

Magaki, S., Hojat, S.A., Wei, B., So, A. and Yong, W.H., 2019. An introduction to the performance of immunohistochemistry. *Biobanking*, pp.289-298.

Majoumouo, M.S., Sharma, J.R., Sibuyi, N.R., Tincho, M.B., Boyom, F.F. and Meyer, M., 2020. Synthesis of biogenic gold nanoparticles from Terminalia mantaly extracts and the evaluation of their in vitro cytotoxic effects in cancer cells. *Molecules*, *25*(19), p.4469.

Mann, R.M., Kuhl, C.K. and Moy, L., 2019. Contrast-enhanced MRI for breast cancer screening. *Journal of Magnetic Resonance Imaging*, *50*(2), pp.377-390.

Martinez-Bosch, N., Vinaixa, J. and Navarro, P., 2018. Immune evasion in pancreatic cancer: from mechanisms to therapy. *Cancers*, *10*(1), p.6.

Mediclinic. The Mediclinic Southern Africa Private Tariff Schedule 2021. Retrieved from: https://www.mediclinic.co.za/content/dam/mc-sa-corporate/downloads/stay-and-visit/Mediclinic%20Southern%20Africa%20Private%20Tariff%20Schedule%202021%20(South%20Africa%20only).pdf. [Accessed on 10/06/2022].

Monticciolo, D.L., Newell, M.S., Moy, L., Niell, B., Monsees, B. and Sickles, E.A., 2018. Breast cancer screening in women at higher-than-average risk: recommendations from the ACR. *Journal of the American College of Radiology*, *15*(3), pp.408-414.

Ngcoza N., 2013. Identification of Biomarkers in Breast Cancer as Potential Diagnostic and Therapeutic agents using a combined in-silico and Molecular Approach. MSc Thesis, UWC - Department of Biotechnology.

Nicolini, A., Ferrari, P. and Duffy, M.J., 2018, October. Prognostic and predictive biomarkers in breast cancer: Past, present and future. In *Seminars in cancer biology* (Vol. 52, pp. 56-73). Academic Press.

Nyante, S.J., Lee, S.S., Benefield, T.S., Hoots, T.N. and Henderson, L.M., 2017. The association between mammographic calcifications and breast cancer prognostic factors in a population-based registry cohort. *Cancer*, *123*(2), pp.219-227.

Ono, T., Kanbayashi, T., Yoshizawa, K., Nishino, S. and Shimizu, T., 2018. Measurement of cerebrospinal fluid orexin-a (hypocretin-1) by enzyme-linked immunosorbent assay: A comparison with radioimmunoassay.

Perrier, A., Gligorov, J., Lefèvre, G. and Boissan, M., 2018. The extracellular domain of Her2 in serum as a biomarker of breast cancer. *Laboratory Investigation*, *98*(6), pp.696-707.

Rajabi, M. and Mousa, S.A., 2017. The role of angiogenesis in cancer treatment. *Biomedicines*, *5*(2), p.34.

Rakha, E.A. and Green, A.R., 2017. Molecular classification of breast cancer: what the pathologist needs to know. *Pathology*, *49*(2), pp.111-119.

Ramos, A.P., Cruz, M.A., Tovani, C.B. and Ciancaglini, P., 2017. Biomedical applications of nanotechnology. *Biophysical reviews*, *9*(2), pp.79-89.

Ratan, Z.A., Zaman, S.B., Mehta, V., Haidere, M.F., Runa, N.J. and Akter, N., 2017. Application of fluorescence in situ hybridization (FISH) technique for the detection of genetic aberration in medical science. *Cureus*, *9*(6).

Rebolj, M., Assi, V., Brentnall, A., Parmar, D. and Duffy, S.W., 2018. Addition of ultrasound to mammography in the case of dense breast tissue: systematic review and meta-analysis. *British journal of cancer*, *118*(12), pp.1559-1570.

Schneider, F., Jin, Y., Van Smaalen, K., Gulbahce, E.H., Factor, R.E. and Li, X., 2019. The FDA-approved breast cancer HER2 evaluation kit (HercepTest; Dako) may miss some HER2-positive breast cancers. *American Journal of Clinical Pathology*, *151*(5), pp.504-510.

Seidel, J.A., Otsuka, A. and Kabashima, K., 2018. Anti-PD-1 and anti-CTLA-4 therapies in cancer: mechanisms of action, efficacy, and limitations. *Frontiers in oncology*, *8*, p.86.

Sharma, A., Boise, L.H. and Shanmugam, M., 2019. Cancer metabolism and the evasion of apoptotic cell death. *Cancers*, *11*(8), p.1144.

Shay, J.W., 2018. Telomeres and aging. *Current Opinion in Cell Biology*, *52*, pp.1-7.

Singh, P., Pandit, S., Mokkapati, V.R.S.S., Garg, A., Ravikumar, V. and Mijakovic, I., 2018. Gold nanoparticles in diagnostics and therapeutics for human cancer. *International journal of molecular sciences*, *19*(7), p.1979.

Sosibo, N.M., Keter, F.K., Skepu, A., Tshikhudo, R.T. and Revaprasadu, N., 2015. Facile attachment of TAT peptide on gold monolayer protected clusters: Synthesis and characterization. *Nanomaterials*, *5*(3), pp.1211-1222.

Sudhakar, A., 2009. History of cancer, ancient and modern treatment methods. *Journal of cancer science & therapy*, *1*(2), p.1.

Sung, H., Ferlay, J., Siegel, R.L., Laversanne, M., Soerjomataram, I., Jemal, A. and Bray, F., 2021. Global cancer statistics 2020: GLOBOCAN estimates of incidence and mortality worldwide for 36 cancers in 185 countries. *CA: a cancer journal for clinicians*, *71*(3), pp.209-249.

Tan, W.C.C., Nerurkar, S.N., Cai, H.Y., Ng, H.H.M., Wu, D., Wee, Y.T.F., Lim, J.C.T., Yeong, J. and Lim, T.K.H., 2020. Overview of multiplex

immunohistochemistry/immunofluorescence techniques in the era of cancer immunotherapy. *Cancer Communications*, *40*(4), pp.135-153.

Tan, X., Oo, M.K.K., Gong, Y., Li, Y., Zhu, H. and Fan, X., 2017. Glass capillary based microfluidic ELISA for rapid diagnostics. *Analyst*, *142*(13), pp.2378-2385.

Tsang, J. and Tse, G.M., 2020. Molecular classification of breast cancer. *Advances in anatomic pathology*, *27*(1), pp.27-35.

Van Amerongen, A., Veen, J., Arends, H.A. and Koets, M., 2018. Lateral flow immunoassays. In *Handbook of Immunoassay Technologies* (pp. 157-182). Academic Press.

Vanderpuye, V., Grover, S., Hammad, N., Simonds, H., Olopade, F. and Stefan, D.C., 2017. An update on the management of breast cancer in Africa. *Infectious agents and cancer*, *12*(1), pp.1-12.

Waldhauer, I. and Steinle, A., 2006. Proteolytic release of soluble UL16-binding protein 2 from tumor cells. *Cancer research*, *66*(5), pp.2520-2526.

Wang, M., Zhang, C., Song, Y., Wang, Z., Wang, Y., Luo, F., Xu, Y., Zhao, Y., Wu, Z. and Xu, Y., 2017. Mechanism of immune evasion in breast cancer. *OncoTargets and therapy*, *10*, p.1561.

Wang, W., Xu, X., Tian, B., Wang, Y., Du, L., Sun, T., Shi, Y., Zhao, X. and Jing, J., 2017. The diagnostic value of serum tumor markers CEA, CA19-9, CA125, CA15-3, and TPS in metastatic breast cancer. *Clinica chimica acta*, *470*, pp.51-55.

Weinberg R., 2007. The nature of cancer. Zayatz E. (ed.), The biology of cancer. Garland Science, Taylor and Francis Group, LLC.

Yamaguchi, K., Chikumi, H., Shimizu, A., Takata, M., Kinoshita, N., Hashimoto, K., Nakamoto, M., Matsunaga, S., Kurai, J., Miyake, N. and Matsumoto, S., 2012. Diagnostic and prognostic impact of serum-soluble UL 16-binding protein 2 in lung cancer patients. *Cancer science*, *103*(8), pp.1405-1413.

Yin, L., Duan, J.J., Bian, X.W. and Yu, S.C., 2020. Triple-negative breast cancer molecular subtyping and treatment progress. *Breast Cancer Research*, *22*(1), pp.1-13.

Zanotel, M., Bednarova, I., Londero, V., Linda, A., Lorenzon, M., Girometti, R. and Zuiani, C., 2018. Automated breast ultrasound: basic principles and emerging clinical applications. *La radiologia medica*, *123*(1), pp.1-12.

Zhang, M., Lee, A.V. and Rosen, J.M., 2017. The cellular origin and evolution of breast cancer. *Cold Spring Harbor perspectives in medicine*, *7*(3), p.a027128.

Zingoni, A., Vulpis, E., Loconte, L. and Santoni, A., 2020. NKG2D ligand shedding in response to stress: role of ADAM10. Frontiers in Immunology, 11, p.447.